



# Seasonal, Diurnal, and Tidal Variations of Dissolved Inorganic Carbon and pCO<sub>2</sub> in Surface Waters of a Temperate Coastal Lagoon (Arcachon, SW France)

Pierre Polsenaere, Bruno Delille, Dominique Poirier, Céline Charbonnier, Jonathan Deborde, Aurélia Mouret, Gwenaël Abril

## ► To cite this version:

Pierre Polsenaere, Bruno Delille, Dominique Poirier, Céline Charbonnier, Jonathan Deborde, et al.. Seasonal, Diurnal, and Tidal Variations of Dissolved Inorganic Carbon and pCO<sub>2</sub> in Surface Waters of a Temperate Coastal Lagoon (Arcachon, SW France). *Estuaries and Coasts*, In press, 10.1007/s12237-022-01121-6 . hal-03797380

**HAL Id: hal-03797380**

**<https://cnrs.hal.science/hal-03797380>**

Submitted on 5 Oct 2022

**HAL** is a multi-disciplinary open access archive for the deposit and dissemination of scientific research documents, whether they are published or not. The documents may come from teaching and research institutions in France or abroad, or from public or private research centers.

L'archive ouverte pluridisciplinaire **HAL**, est destinée au dépôt et à la diffusion de documents scientifiques de niveau recherche, publiés ou non, émanant des établissements d'enseignement et de recherche français ou étrangers, des laboratoires publics ou privés.

# **Seasonal, diurnal and tidal variations of dissolved inorganic carbon and pCO<sub>2</sub> in surface waters of a temperate coastal lagoon (Arcachon, SW France)**

Pierre Polsenaere<sup>1,2\*</sup>, Bruno Delille<sup>3</sup>, Dominique Poirier<sup>1</sup>, Céline Charbonnier<sup>1</sup>, Jonathan Deborde<sup>1,2</sup>, Aurélia Mouret<sup>1,4</sup> and Gwenaél Abril<sup>1,5,6</sup>

\*Corresponding author: Pierre.Polsenaere@ifremer.fr

<sup>1</sup> Laboratoire Environnements et Paléoenvironnements Océaniques et Continentaux (EPOC), CNRS-UMR 5805, Université de Bordeaux, France.

<sup>2</sup> IFREMER, Littoral, Laboratoire Environnement et Ressources des Pertuis Charentais (LER-PC), BP133, 17390, La Tremblade, France.

<sup>3</sup> Unité Océanographie Chimique, Département d'Astrophysique, Géophysique et Océanographie, Université de Liège, Allée du 6 Août, 17-Bât. B5 4000 Liège, Belgium.

<sup>4</sup> UMR 6112 LPG-BIAF Recent and Fossil Bio-Indicators, Angers University, 2 Bd Lavoisier, F-49045, Angers, France.

<sup>5</sup> Laboratoire de Biologie des Organismes et Écosystèmes Aquatiques (BOREA), UMR CNRS 8067, Muséum National d'Histoire Naturelle, 61 rue Buffon, 75231, Paris cedex 05, France.

<sup>6</sup> Programa de Biologia Marinha e Ambientes Costeiros, Universidade Federal Fluminense, Outeiro São João Batista s/n, 24020015, Niterói, RJ, Brazil.

**A research paper published in Estuaries and Coasts**

Key words: coastal zone; dissolved inorganic carbon; water pCO<sub>2</sub>; water-air CO<sub>2</sub> fluxes; tidal, diurnal, seasonal variations; physical, biological, chemical processes.

## Abstract

We report on diurnal, tidal and seasonal variations of dissolved inorganic carbon (DIC), water partial pressure of CO<sub>2</sub> (pCO<sub>2</sub>) and associated water-air CO<sub>2</sub> fluxes in a tidal creek of a temperate coastal lagoon with 70 % of intertidal flats, during eight tidal/diurnal cycles and two consecutive years covering all seasons. Surface waters of the lagoon were always slightly oversaturated in CO<sub>2</sub> with respect to the atmosphere with an average pCO<sub>2</sub> value of  $496 \pm 36$  ppmv. Seasonally, subsurface water pCO<sub>2</sub> values were controlled by both temperature and biological / tidal advection effects that compensated each other and resulted in weak annual variations. High-resolution temporal pCO<sub>2</sub> records reveal that highest fluctuations (192 ppmv) occurred at the tidal/diurnal scale as a result of biological activity, advection from the tidal flat and porewater pumping that all contributed to water pCO<sub>2</sub> and carbonate chemistry variations. Total Alkalinity (TA) versus salinity plots suggest a net production of alkalinity in the lagoon attributed to benthic carbonate dissolution and/or anaerobic degradation of organic matter. We specifically highlighted that for a same salinity range, during flooding, daytime pCO<sub>2</sub> were generally lower than nighttime pCO<sub>2</sub> values because of photosynthesis, whereas during ebbing, daytime pCO<sub>2</sub> were higher than nighttime pCO<sub>2</sub> values because of heating. Waters in the lagoon were a relatively weak CO<sub>2</sub> source to the atmosphere over the year compared to other estuarine and lagoon waters elsewhere, and to sediment-air fluxes measured simultaneously by atmospheric Eddy Covariance (EC) in the Arcachon lagoon. Because of low values and small variations of the air-sea pCO<sub>2</sub> gradient, the variability of fluxes calculated using the piston velocity parameterization was greatly controlled by the wind speed at the diurnal and, to a lesser extent, seasonal time scales. During the emersion, the comparison of these pCO<sub>2</sub> data in the tidal creek with EC fluxes measured 1.8 km away on the tidal flat suggests high heterogeneity in air-sea CO<sub>2</sub> fluxes, both spatially and at short time scales according to the inundation cycle

and the wind speed. In addition to tidal pumping when the flat becomes emerged, our data suggest that lateral water movement during the emersion of the flat generates strong spatial heterogeneity in water-air CO<sub>2</sub> flux.

## **1. Introduction**

Coastal zones represent key systems in biogeochemical cycle couplings between land, oceans and the atmosphere, processing considerable amounts of matter, energy and nutrients (Borges et al. 2005; Cole et al. 2007; Cai 2011). Despite its relatively modest surface area (7 % of the global ocean surface), the coastal zone accounts for 14-30 % of all oceanic primary production and 90 % of sedimentary organic carbon mineralization (Gattuso et al. 1998; Mantoura et al. 1991; Pernetta and Milliman 1995). Carbon fluxes within and between coastal subsystems and their alteration by climate and anthropogenic changes are substantial. It is essential to understand and accurately account for the factors regulating these fluxes and how they affect the ocean and global carbon budgets (Bauer et al. 2013).

The coastal ocean consists of different but tightly connected ecosystems including estuaries, tidal wetlands, lagoons and the continental shelf. Global CO<sub>2</sub> emissions from estuaries have been estimated at 0.2-0.4 Pg yr<sup>-1</sup> (Cai 2011; Borges and Abril 2011; Borges et al. 2005; Laruelle et al. 2010), with fluxes disproportionally high in comparison with their global ocean area portion (near 0.2 %). To the contrary, other coastal systems such as tidal wetlands and continental shelves fix 0.55 and 0.25 Pg yr<sup>-1</sup> of atmospheric CO<sub>2</sub> respectively (Bauer et al. 2013). The spatiotemporal heterogeneity and complexity of coastal systems in terms of carbon processes and fluxes make difficult to precisely quantify each sub-system's carbon balance. For instance, carbon fluxes in tidal systems such as estuaries and small deltas are relatively well characterized (Laruelle et al. 2010; Borges and Abril 2011; Chen et al. 2013). To the contrary, other systems such as fjords, lagoons and marine embayments are neglected despite a large

relative surface among coastal systems, a generally high net primary production and a strong sensitivity to eutrophication phenomenon (Kjerfve 1985; Caumette et al. 1996; Koné et al. 2009; Polsenaere et al. 2012a; Cotovicz et al. 2015). As a consequence, carbon flux measurements are needed for an accurate estimate of global and regional carbon budgets.

In coastal ecosystems, dissolved inorganic carbon (DIC) concentrations, and particularly partial pressures of CO<sub>2</sub> (pCO<sub>2</sub>) are driven by several thermodynamic and biotic factors, induced by river water inputs, tidal exchanges, mixing of water masses, photosynthesis and aerobic/anaerobic degradation of organic matter, precipitation/dissolution of calcium carbonate, benthic/pelagic couplings and air-water exchanges (Cai 2011; Gazeau et al. 2004; Cotovicz et al. 2015; Ribas-Ribas et al. 2011). Efforts have been made to understand the seasonal and inter-annual processes affecting carbon system dynamics over coastal ecosystems (Yates et al. 2007). Seasonal measurements of the carbonate system parameters (pCO<sub>2</sub>, Total Alkalinity, DIC, and/ or pH) have been performed for instance across salinity gradient transects or strategically located stations along lagoon channels or estuaries (Frankignoulle et al. 1996; Cai et al. 1999; Koné et al. 2009; Ribas-Ribas et al. 2011; Burgos et al. 2018; Wang et al. 2018; Vaz et al. 2019). The influence of smaller-scale rhythms (tidal and diurnal variations) on seasonal and annual carbon dynamics and budgets has also been studied through direct diurnal cycles for instance over east monsoon coastal systems and subtropical bays (Dai et al. 2009; Yates et al. 2007), temperate sea, lagoon, estuary, river, channel and creek (Saderne et al. 2013; Bozec et al. 2011; Borges and Frankignoulle 1999; Ribas-Ribas et al. 2013; Burgos et al. 2018), sub-Antarctic island coastal waters (Delille et al. 2009), tropical and equatorial mangrove waters (Maher et al. 2013; Bouillon et al. 2007; Borges et al. 2003) and continental and subtropical saltmarsh and marsh-dominated estuary systems (Wang and Cai, 2004; Wang et al. 2016; Wang et al. 2018). For instance, in a tidal creek among the Duplin River salt marsh-estuary coastal ecosystem (Georgia, USA), Wang et al. (2018) measured strong seasonal and

75 tidal/diurnal pCO<sub>2</sub> variations with values ranging from 500 ppmv at high tide to 4000 ppmv at  
76 low tide and to 1600 ppmv at high tide to 12,000 ppmv at low tide during coldest and warmest  
77 months, respectively. Horizontal advection with river water entrance to the creek at high tide  
78 was mentioned to explain lower measured values. To the contrary, for higher values observed  
79 at low tide, creek bank pore-water drainage associated to tidal pumping process, as observed  
80 over mangroves or wetlands (Maher et al. 2013; Neubauer and Anderson 2003) was highlighted  
81 (Wang et al. 2018). Over tidally-influenced shallow systems, all these processes are generally  
82 but differently involved and can in turn significantly and specifically influence atmospheric  
83 CO<sub>2</sub> fluxes.

84 CO<sub>2</sub> fluxes at the water-air interface can be measured directly using the Eddy Covariance  
85 (Zemmelink et al. 2009; Polsenaere et al. 2012a), floating chambers (Frankignoulle et al. 1998)  
86 or be calculated from water pCO<sub>2</sub> measurements and a given gas transfer velocity. CO<sub>2</sub> flux  
87 computations can be subject to large uncertainties because of the difficulty in accurately  
88 assessing the gas transfer velocity (Raymond and Cole 2001, Vachon et al. 2010). This bias is  
89 potentially more important when the water-air CO<sub>2</sub> gradient is small. Diurnal and tidal  
90 variations in water pCO<sub>2</sub> of dynamic coastal ecosystems can even add uncertainties on air-sea  
91 CO<sub>2</sub> flux estimations. For example, in the Guadalquivir estuary, Ribas-Ribas et al. (2013)  
92 observed pCO<sub>2</sub> values fluctuating from source to sink over the same tidal cycle.

93 In the present study we report tidal, diurnal and seasonal dynamics of inorganic carbon and  
94 associated air-sea CO<sub>2</sub> fluxes in a tidal creek of the temperate coastal Arcachon lagoon (SW  
95 France). The lagoon is a typical tidal flat of the French Atlantic coast subjected to both marine  
96 and continental influences. A complex channel and tidal creek waters network drains the tidal  
97 flat during ebb tides. Tidal pumping through anoxic pore-water seeping from mud sediments to  
98 tidal creek waters is an important component of the biogeochemical functioning of the lagoon  
99 in terms of nutrient dynamics (Deborde et al., 2008a). In this paper, DIC parameters and

associated water-air CO<sub>2</sub> fluxes as estimated based on several *in situ* tidal/diurnal cycles (six 24-hour and two 12-hour cycles) carried at different seasons during two years (2008 and 2009) are presented. We describe and explain small-scale (diurnal and tidal) and seasonal pCO<sub>2</sub> variability along with relevant environmental controls in studied tidal creek waters. We compute air-sea CO<sub>2</sub> fluxes, and discuss associated variability according to small (diurnal and tidal) and seasonal scales and also methodology from coastal regional/global carbon budgets point of view. The computed water-air CO<sub>2</sub> fluxes estimated during these tidal/diurnal cycles are also compared with those measured in summer 2008 by atmospheric Eddy Covariance (EC) over the tidal flat (Polsenaere et al. 2012a).

## **2. Materials and Methods**

### **2.1. Study area**

The Arcachon bay is a temperate macro-tidal lagoon of 174 km<sup>2</sup> on the southwestern Atlantic coast of France (44°40' N, 01°10' W) (Fig. 1). Several studies have focused on the system in particular its hydrodynamics through modelling simulations (Plus et al. 2009; Fauvelle et al. 2018); *Zostera* seagrass meadow dynamic (Auby and Labourg 1996; Plus et al. 2010; Cognat et al. 2018) and relationships with sediment hydrodynamics or redox status (Ganthy et al. 2013; Delgard et al. 2013; Deborde et al. 2008a,b); nutrient and carbon dynamics and export from the Arcachon catchment through *in situ* adapted sampling and modelling strategies (Auby et al. 1994; Rimmelin et al. 1998; Canton et al. 2012; Polsenaere et al. 2012b; Polsenaere and Abril 2012); and in terms of benthic and pelagic primary production measurements through various *in situ*, laboratory and modelling approaches (Polsenaere et al. 2012a; Migné et al. 2016; Glé et al. 2008; Plus et al. 2015).

This triangle-shaped bay is surrounded by the coastal plain of the *Landes de Gascogne*, and communicates with the Atlantic Ocean through a narrow channel 8 km in length (Fig. 1). With

a mean depth of 4.6 m, the shallow lagoon presents semi-diurnal tides with amplitudes varying from 0.8 to 4.6 m (Plus et al. 2009). During a tidal cycle, the flat exchanges approximately  $264 \times 10^6 \text{ m}^3$  and  $492 \times 10^6 \text{ m}^3$  of water with the ocean, respectively during average neap and spring tides. The flushing time of the lagoon ranges between 12.4 and 17.4 days in winter and summer respectively (Plus et al. 2009). Water temperatures in the lagoon vary from 6 °C in winter to 22.5 °C in summer, and water salinity varies from 22 to 35 according to freshwater input variations during the year.

The flats are tidally submerged by relatively saline waters, and receive moderate amounts of freshwater with an annual input of  $813 \times 10^6 \text{ m}^3$  ( $1.8 \times 10^6 \text{ m}^3$  at each tidal cycle), of which 8 % is from groundwater, 13 % is from rainfall and 79 % is from rivers and small streams (Rimmelín et al. 1998). In total, the carbon export from the watershed to the Arcachon lagoon was estimated at  $15,870 \text{ t C yr}^{-1}$  or  $6 \text{ t C km}^{-2} \text{ yr}^{-1}$ , mostly in the form of dissolved organic carbon (DOC) (35 %), DIC (24 %) as excess  $\text{CO}_2$  and  $\text{DIC}_{\text{equilibrium}}$  (i.e. the theoretical DIC concentration at the atmospheric equilibrium), and dissolved  $\text{CO}_2$  rapidly lost as degassing to the atmosphere (34 %) (Polsenaere et al. 2012b). Tidal pore-water drainage at low tide is not documented for carbon, but contributes to respectively 55 and 15 % of the dissolved inorganic phosphate (DIP) and nitrate (DIN) input to the lagoon waters (Deborde et al. 2008a).

The lagoon surface is composed of  $57 \text{ km}^2$  of channels (33 % of the lagoon surface area), with a maximum depth of 25 m at the mouth of the lagoon. These channels drain a large muddy tidal flat of  $117 \text{ km}^2$  (67 % of the lagoon). *Zostera noltei* seagrass beds are particularly extensive and colonize up to 60 % of this intertidal area (i.e.  $70 \text{ km}^2$ ) between  $-1.9 \text{ m}$  and  $+0.8 \text{ m}$  relative to local Mean Sea Level (Amanieu, 1967). Annual mean net primary production of *Zostera noltei* expressed as carbon fixation was estimated at  $362.9 \pm 88.1 \text{ t C km}^{-2} \text{ yr}^{-1}$  (Ribaudou et al. 2017). Polsenaere et al. (2012a) and Migné et al. (2016) gave annual values of the same order of magnitude through atmospheric EC and benthic chamber measurements with 456 and 263 t C



km<sup>-2</sup> yr<sup>-1</sup> respectively. However, seagrass beds in the lagoon declined by 33 % since the end of the 80's whereas the exact causes remain unclear, leading to a C fixation decline from 24846 ± 6030 t C yr<sup>-1</sup> (1989) to 16564 ± 4020 t C yr<sup>-1</sup> (2007) (Plus et al. 2009; Plus et al. 2015; Ribaud et al. 2017). The microphytobenthic (MPB) communities also represent a significant proportion of the total benthic primary production, which is estimated at between 104-114, 628 and 788 t C km<sup>-2</sup> yr<sup>-1</sup> (Auby personal communication; Polsenaere et al. 2012a; Migné et al. 2016). Together, these two categories of benthic primary production represent more than half of the total primary production of the flat. Annual integrated phytoplankton primary production has been estimated at 103 t C km<sup>-2</sup> yr<sup>-1</sup> which could represent 30 % of the total primary production of the lagoon and places Arcachon within the low to moderate phytoplankton primary production systems (Glé et al. 2008). Microphytobenthic resuspension is also supposed to significantly contribute to planktonic production in Arcachon as highlighted by Savelli et al. (2019) on the Brouage mudflat of the Marennes-Oléron Bay up North along the French Atlantic coast with a 43 % resuspended MPB primary production at this location. The presence of circular tidal pools on the flat also contributes to the biogeochemical functioning of Arcachon bay especially at tidal and diurnal scales (Rigaud et al. 2018) through large spatio-temporal variations in water temperature and irradiance influencing MPB activity and benthic oxygen, nutrients, and reduced compound fluxes.

Finally, net CO<sub>2</sub> fluxes between the lagoon and the atmosphere measured at the ecosystem scale by atmospheric EC generally showed small negative (influx) and positive (efflux) values (-13 μmol m<sup>-2</sup> s<sup>-1</sup> for influxes and 19 μmol m<sup>-2</sup> s<sup>-1</sup> for effluxes). Emersion during the day was almost always associated with a net uptake of atmospheric CO<sub>2</sub> due to an enhanced benthic primary production at low tide. In contrast, during immersion (day and night) and emersion at night, CO<sub>2</sub> fluxes were positive, negative or close to zero, depending on the season and the study site (Polsenaere et al. 2012a).

## 2.2. Sampling strategy and laboratory analysis

In total, six 24-hour cycles (April, July, September 2008, and April, June and September 2009) and two 12-hour cycles (November 2008 and January 2009) were carried out in a subtidal creek at the centre of the lagoon (Fig. 1). For each cycle, water height (H), salinity (S), temperature (T), partial pressure of CO<sub>2</sub> in the water (pCO<sub>2</sub>), total alkalinity (TA) and dissolved inorganic carbon isotopic ratio ( $\delta^{13}\text{C-DIC}$ ) were measured at the subsurface (0.5 m depth). T and S were measured every minute with an YSI multiparameter probe on board and H was measured every hour by the SHOM (Service Hydrographique et Océanographique de la Marine) at Arcachon (Eyrac pier, 44°39.9001'N 01°09.8130'W). Before each cycle, the salinity (conductivity) sensor was checked and calibrated with 10 and 50 mS cm<sup>-1</sup> solutions. Water pCO<sub>2</sub> was measured every minute with a marble-type equilibrator system (Frankignoulle et al. 2001; Polsenaere et al. 2012b). An Infra-Red Gas Analyzer (LI-COR, LI-820) was used to measure the pCO<sub>2</sub> in dry air equilibrated with seawater. The LI-820 was calibrated at the laboratory one day before the field experiment using three gas standards of 0, 500 ± 10 ppm and 2959 ± 59 ppm. The equilibrator consists of a Plexiglas cylinder (height: 90 cm, diameter: 16 cm) that is filled with marbles to increase the exchange surface area. Water pumped by a peristaltic pump (Masterflex, 1 L min<sup>-1</sup>), runs from the top to the bottom of the equilibrator, and air is pumped upwards (1 L min<sup>-1</sup>). The pCO<sub>2</sub> of air equilibrates with the pCO<sub>2</sub> of water and is then measured by the LI-COR after being dried by a Dierite grain tube. Response time of the equilibrator as determined in the laboratory is shorter than 5 minutes (Cotovicz et al. 2016).

Discrete water samples were also taken every hour of the tidal cycle for TA and  $\delta^{13}\text{C-DIC}$  in the channel subsurface waters by using a 5L Niskin sampler. Total alkalinity (TA) was measured by titration with HCl 0.1 N on 100 mL filtered samples and was calculated by a Gran function linearisation (Gran 1952) between pH 4.2 and 3. The reproducibility between the measures was better than ±5 µmol kg<sup>-1</sup>. Accuracy of TA measurements was checked on regular

200 titrations of a secondary standard of 0.2  $\mu\text{m}$  filtered seawater with a well-known TA  
201 concentration, previously calibrated by comparison with a standard from Scripps Institution of  
202 Oceanography. The  $\delta^{13}\text{C}$ -DIC measurements were made following Gillikin and Bouillon  
203 (2007). In 100 mL vials that were filled to the top, a headspace was first created with Helium  
204 gas to obtain a volume of approximately 20 % of the total volume of the vial. Then, 0.3 mL of  
205 warm 85 % phosphoric acid was added to transform the carbonate forms into  $\text{CO}_2$ . To ensure  
206 gas equilibration, the vials were shaken and placed upside down for 1.5 h. Measurements were  
207 performed by coupling an elemental analyzer (EA; Carlo Erba NC2500) to an Isotope Ratio  
208 Mass Spectrometer (IRMS; Micromass Isoprime) equipped with a manual gas injection. We  
209 injected 3 mL of headspace gas from the vial headspace.  $\delta^{13}\text{C}$ -DIC was calibrated against a  
210 laboratory standard (45 mg of  $\text{Na}_2\text{CO}_3$  were dissolved in a sealed vial flushed with He gas, with  
211 3 mL of warm 85 % phosphoric acid  $\text{H}_3\text{PO}_4$ ). This standard had been calibrated against a  
212 certified standard (NBS19, -1.96 ‰) using a dual-inlet IRMS. The isotopic value of the standard  
213  $\text{Na}_2\text{CO}_3$  was  $-4.5 \pm 0.2$  ‰. Finally, the equation of Miyajima et al. (1995) was applied to correct  
214 for the isotopic fractionation of the  $\text{CO}_2$  between the headspace and the water phase and to  
215 calculate the  $\delta^{13}\text{C}$  of the total DIC. The repeatability was approximately  $\pm 0.1$  ‰ between  
216 samples. The stable isotopic composition of DIC ( $\delta^{13}\text{C}$ -DIC) varies over a large range in  
217 terrestrial and coastal waters since carbon reservoirs that act as a source of DIC (soil,  
218 groundwater, bedrocks and atmosphere) have distinct isotopic signatures (Yang et al. 1996).  
219 The  $\delta^{13}\text{C}$  of atmospheric  $\text{CO}_2$  is about -7.5 ‰, whereas carbonate rocks have a  $\delta^{13}\text{C}$  of about 0  
220 ‰ (Mook et al. 1983). In a system where soil  $\text{CO}_2$  is primarily derived from decomposition of  
221 plant organic matter, the  $\text{CO}_2$  produced has a  $\delta^{13}\text{C}$ - $\text{CO}_2$  value close to the initial substrate (i.e.,  
222 -30 to -24 ‰ in the case of C3 plants and -16 to -10 ‰ in the case of C4 plants). Aquatic  
223 primary production, in contrast, tends to increase  $\delta^{13}\text{C}$ -DIC and generate strong diel variations

(Parker et al. 2005). Finally, gas exchange along subsurface waters generates an isotopic equilibration with the atmosphere and makes the  $\delta^{13}\text{C}$ -DIC less negative.

### 2.3. Calculations and statistical analysis

Dissolved inorganic carbon (DIC) concentrations and species (bicarbonate  $\text{HCO}_3^-$  and carbonate  $\text{CO}_3^{2-}$  ions) were calculated from the measured salinity, temperature,  $\text{pCO}_2$  and TA using the carbonic acid constants sets from Mehrbach et al. (1973) as modified by Dickson and Millero (1987), the borate acidity constant from Lee et al. (2010), the  $K_{\text{HSO}_4}$  constant from Dickson (1990) and the  $\text{CO}_2$  solubility coefficient of Weiss (1974). The  $\text{CO}_2$  System Calculation program (version 2.1.) developed by Lewis and Wallace (1998) performed all calculations.

Seasonal temperature ( $\text{TpCO}_2$ ) versus non-temperature ( $\text{NpCO}_2$ ) effects on measured water  $\text{pCO}_2$  during the eight tidal cycles were studied applying equations from Takahashi et al. (2002) as follows:

$$\text{TpCO}_2 = \text{pCO}_{2\text{mean}} \times \exp[0.0423(\text{T}_{\text{obs}} - \text{T}_{\text{mean}})] \quad (1)$$

$$\text{NpCO}_2 = \text{pCO}_{2\text{obs}} \times \exp[0.0423(\text{T}_{\text{mean}} - \text{T}_{\text{obs}})] \quad (2)$$

Where  $\text{pCO}_{2\text{obs}}$ ,  $\text{T}_{\text{obs}}$ ,  $\text{pCO}_{2\text{mean}}$ ,  $\text{T}_{\text{mean}}$  are respectively the measured  $\text{pCO}_2$ , temperatures at each time step and the annual mean  $\text{pCO}_2$  and temperature calculated across the whole measured dataset.  $\text{TpCO}_2$  indicates the  $\text{pCO}_2$  variations around the mean  $\text{pCO}_2$  that would be expected only from temperature fluctuations that occurred over the sampling period (2008-2009).  $\text{NpCO}_2$  represent  $\text{pCO}_2$  variations due to biological activity or non-temperature effects (advection, tidal pumping and benthic-pelagic coupling). The constant 0.0423 corresponds to the temperature effect on  $\text{pCO}_2$  in isochemical conditions ( $\text{qln pCO}_2/\text{qT}$ ), i.e.  $+4.23 \text{ \% } ^\circ\text{C}^{-1}$ .

Gas transfer velocities ( $k_{600}$ ) and air-sea  $\text{CO}_2$  fluxes for the eight tidal cycles were computed each hour at high-tide day and night periods. Wind speed values normalized to a 10 meters

height ( $U_{10}$ ) values were computed from wind speed values measured at 9 meters high by the Lège-Cap Ferret Meteo-France station (44°37.900'N 01°14.900'W, 12.5 km far from the 24-H site, Fig. 1) using the Amorochio and DeVries (1980) equation. Gas transfer velocities ( $k$ ) were estimated according to parameterizations of Wanninkhof et al. (1992), Raymond and Cole (2001) and Abril et al. (2009), noted W92, RC01 and A09, respectively. The W92 equation has been proposed for oceanic water, whereas the RC01 and A09 equations were developed for estuarine waters. For the latter equation, hourly suspended particulate matter (SPM) concentrations measured during every cycle (data not shown) and bottom water velocity currents estimated with the hydrodynamic model from Ifremer (MARS3D, Lazure and Dumas, 2008) were used. Air-sea  $CO_2$  fluxes were then calculated from  $k$ , water and air  $pCO_2$  values. The gas transfer coefficients normalized to a Schmidt number of 600 ( $k_{600}$ ) estimated with the three parameterizations were converted to the gas transfer velocity of  $CO_2$  ( $k$ ) at *in situ* temperature and salinity following the procedure of Jähne et al. (1987). Air-water  $CO_2$  fluxes were estimated using the formulation as followed:

$$F_{CO_2} = \alpha k \Delta pCO_2 \quad (3)$$

where  $F_{CO_2}$  is the vertical  $CO_2$  exchange at the air-water interface,  $\alpha$  is the  $CO_2$  solubility coefficient (Weiss 1974),  $k$  is the gas transfer velocity, and  $\Delta pCO_2$  is the gradient between water  $pCO_2$  measured by the equilibrator and air  $pCO_2$  set to a mean value of 390 ppm according to simultaneous Eddy Covariance (EC) measurements done in the lagoon (44°42.9858'N 01°08.6160'W, 1.829 km far from the 24-H site, Fig. 1) in 2008 and 2009 (Polsenaere et al. 2012a). For comparison,  $U_{10}$  and air-sea  $CO_2$  flux values obtained in July 2008 from simultaneous EC measurements (Polsenaere et al. 2012a) and water carbon parameters ( $pCO_2$ ) during the July 2008 cycle are also presented.

Data post-processing (graphs and statistics) was performed using the GraphPad Prism version 6.00 software (La Jolla California USA, [www.graphpad.com](http://www.graphpad.com)). The Shapiro-Wilk test was used

to test the normality of the data (p-value below 0.05). Due to non-normality of our data, Mann-Whitney and Kruskal-Wallis (p-value below 0.05) were performed to detect significant differences in carbon and associated parameters between tidal/diurnal cycles (seasons) and also across diurnal and tidal rhythms (emersion around low tide during the day (LT/Day), emersion at night (LT/Night), immersion around high tide during the day (HT/Day) and immersion at night (HT/Night)) (emersion and immersion periods last during 4 and 8 hours twice per day in the Arcachon lagoon). The Dunn's post-hoc multiple comparisons' test to Kruskal-Wallis was chosen to detect significant differences among groups.

### **3. Results**

#### **3.1. Water pCO<sub>2</sub> and associated parameter temporal variations**

##### ***3.1.1. At the seasonal time scale***

In 2008/09 at our 2.5 meter deep (on average, hydrographic zero) subtidal creek in the Arcachon lagoon, water temperatures averaged  $17.7 \pm 4.2$  °C over the years 2008 and 2009 and ranged between  $8.9 \pm 0.4$  °C in January 2009 and  $22.2 \pm 0.6$  °C in July 2008 (Table 1, Fig. 2). Water mean salinity value was  $30.5 \pm 3.4$  with a particularly low mean value measured in January 2009 (Table 1,  $23.2 \pm 1.5$ , Fig. 3).

Bicarbonates (HCO<sub>3</sub><sup>-</sup>), carbonates (CO<sub>3</sub><sup>2-</sup>) and the sum of dissolved CO<sub>2</sub> and carbonic acid H<sub>2</sub>CO<sub>3</sub> concentrations (CO<sub>2</sub><sup>\*</sup>) represented respectively 91 to 95 %, 3 to 8 % and about 1 % of the whole DIC (data not shown). TA values followed DIC patterns with a lowest mean value of  $1.646 \pm 0.086$  mmol kg<sup>-1</sup> in January 2009 and a highest mean value  $2.255 \pm 0.021$  mmol kg<sup>-1</sup> in September 2008 (Fig. 3, Table 1). δ<sup>13</sup>C-DIC mean values were close to 0 ‰ and ranged between  $-1.1 \pm 1.1$  ‰ in April 2008 (minimum values in winter/spring) and  $-0.2 \pm 0.2$  ‰ in June 2009 (maximum values in summer/autumn). Particularly low negative values up to -3.7 ‰ were measured in April 2008 (Table 1, Fig. 3). Over the whole studied period, global

299 significant and positive TA, DIC and  $\delta^{13}\text{C}$ -DIC values versus salinity values were obtained  
 300 ( $\text{TA}=0.05143*\text{S} + 0.5079$ ,  $\text{R}^2$ : 0.88;  $\text{DIC}=0.03815*\text{S} + 0.7594$ ,  $\text{R}^2$ : 0.82;  $\delta^{13}\text{C}\text{-DIC}=0.08697*\text{S}$   
 301  $- 3.284$ ,  $\text{R}^2$ : 0.15;  $p<0.0001$ , Fig. 4a, c, d). At each cycle (season) apparent 0 end-member TA  
 302 and *in situ* catchment TA values were computed from the Y-intercept of TA versus S cross-  
 303 correlations (Fig. 4a) and *in situ* TA measurements carried out at the same time over the  
 304 Arcachon lagoon watershed watercourses (Polsenaere et al. 2012b) calculated here as  
 305 discharge-weighted TA means, respectively (Fig. 4b). Apparent 0 end-member TA values were  
 306 generally higher than *in situ* catchment values except during the end of summer and autumn  
 307 period (September and November 2008, Fig. 4b).  
 308 Water  $\text{pCO}_2$  averaged  $496 \pm 36$  ppmv over the sampling years and were always oversaturated  
 309 whatever the season and period of the day and tide, with regards to the atmospheric equilibrium  
 310 of 390 ppmv (Figs. 2, 3, 5, Table 1). Mean values ranged from  $461 \pm 14$  ppmv in July 2008 to  
 311  $530 \pm 39$  ppmv in September 2009 (minimum and maximum values in summer/autumn) with  
 312 in general (except between November and July 2008 and between April and September 2009)  
 313 only significant differences between seasons (Kruskal-Wallis test,  $p<0.05$ ) though lower than  
 314 those observed at the diurnal/tidal scale (Table 1, Figs. 2, 3, 5).  
 315 Seasonal variations in *in situ* measured temperature,  $\text{pCO}_2$  values and in temperature ( $\text{TpCO}_2$ ,  
 316  $\text{tpCO}_2$ ) versus non-temperature ( $\text{NpCO}_2$ ) effects on  $\text{pCO}_2$  are presented in Figure 2. During  
 317 2008,  $\text{pCO}_2$  values showed weak seasonal variations increasing from April 2008 ( $474 \pm 14$   
 318 ppmv) to September 2008 ( $515 \pm 36$  ppmv) before decreasing towards November 2008 ( $463$   
 319 ppmv). In 2009,  $\text{pCO}_2$  increased from January to April ( $525 \pm 14$  ppmv) before decreasing  
 320 towards June ( $490 \pm 27$  ppmv) and increasing again to September ( $530 \pm 39$  ppmv, Table 1,  
 321 Fig. 2) as in 2008. In 2008,  $\text{NpCO}_2$  values showed larger seasonal variations first decreasing  
 322 from April to July ( $557 \pm 22$  and  $381 \pm 16$  ppmv respectively), and then increasing towards  
 323 November ( $583 \pm 27$  ppmv). To the contrary in 2009, a decrease was first observed from

January ( $698 \pm 16$  ppmv) to June 2009 ( $417 \pm 24$  ppmv) before increasing towards September ( $463 \pm 37$  ppmv). In 2008 and 2009 respectively,  $\text{TpCO}_2$  followed exactly the opposite patterns. Peak-to-peak seasonal amplitudes in *in situ* temperature and  $\text{pCO}_2$  values were  $9.9^\circ\text{C}$  and 52 ppmv in 2008 and  $12.6^\circ\text{C}$  and 50 ppmv in 2009 (Fig. 2, Table 1).

### 3.1.2. At the diurnal/tidal time scales

Significant variations in inorganic carbon and associated parameters occurred at the diurnal/tidal scales (Table 1, Figs. 2, 3, 5). Water heights ranged from 0.4 m (July 2008 and June 2009) at low tide to 4.5 m (July 2008, January and June 2009) at high tide (Fig. 3). The largest salinity variation occurred during winter and spring with for instance 5.2 and 6.7 salinity unit difference between low and high tides in January and April 2009 respectively. During these seasons, at low tide, the lowest salinity values of 20.4 and 24.8 respectively were observed. To the contrary, during summer and autumn seasons, salinity values were higher (minimum values 30.2 at low tide in July 2008 and June 2009) and varied by less than 2.4 units throughout the tidal cycle (Table 1, Figs. 3, 5). Water temperature variations at the tidal/diurnal scales were small and ranged from  $1.4/1.3^\circ\text{C}$  in September 2008/2009 to  $3.3^\circ\text{C}$  in June 2009 (Table 1, Figs. 3, 5).

With regards to inorganic carbon parameters, DIC and TA concentrations showed weak diurnal/tidal variations with significant differences between high and low tides except in September 2008 (ranges of  $0.078\text{ mmol kg}^{-1}$  for TA and  $0.069\text{ mmol kg}^{-1}$  for DIC) and in June 2009 where lower values were measured during low tide periods, concomitant to lower salinities.  $\delta^{13}\text{C}$ -DIC values were significantly higher during high tide in July 2008 and June 2009 (ranges:  $-1.7$  to  $0.2\text{ ‰}$  and  $-0.4$  to  $0.2\text{ ‰}$ , respectively) (Table 1, Fig. 3).

Water  $\text{pCO}_2$  tidal/diurnal variations ranged between 50 ppmv in winter and spring (51 and 54 ppmv in January 2009 and April 2008 respectively) to 150-200 ppmv in summer and autumn (148 and 192 ppmv in September 2009 and 2008) (Figs. 2, 3, 5). Whatever the season and hour,



349 water pCO<sub>2</sub> values were always oversaturated compared to the atmospheric value of 390 ppm;  
 350 at minimum over all tidal/diurnal cycles, pCO<sub>2</sub> value dropped to 405 ppmv in September 2008)  
 351 (Table 1, Figs. 2, 3, 5). Some significant pCO<sub>2</sub> variations also occurred in the creek between  
 352 nighttime and daytime and between the emersion and the immersion of the tidal flat (LT\_D,  
 353 LT\_N, HT\_D and HT\_N periods, see Fig. 5 caption and M&M section) (Non-parametric Mann-  
 354 Whitney test,  $p < 0.05$ ) (Figs. 3 and 5, Table 1). In winter-spring (April 2008, November 2008,  
 355 January 2009 and April 2009), during daytime pCO<sub>2</sub> were significantly higher and daytime  
 356 salinity were lower than at night. To the contrary, in summer-autumn (July 2008, September  
 357 2008/09 and June 2009), daytime pCO<sub>2</sub> values were significantly lower than nighttime pCO<sub>2</sub>  
 358 and salinity were higher at night. During the eight cycles, pCO<sub>2</sub> values at low tide were  
 359 significantly higher than values at high tide (salinity values at low tide were also below high  
 360 tide values) (Figs. 2, 3, 5, Table 1).

361 A correlation analysis showed significant negative correlations between water pCO<sub>2</sub> and  
 362 salinity (or water height) values (i.e. Spearman coefficients pCO<sub>2</sub> versus salinity of -0.69 and -  
 363 0.92,  $p < 0.01$  in July 2008 and September 2009 respectively), except in September and  
 364 November 2008 (Fig. 3). pCO<sub>2</sub> values were also negatively correlated to  $\delta^{13}\text{C}$ -DIC values in  
 365 July 2008 and over all 2019 cycles ( $R$ : -0.63, -0.72 and -0.58 in July 2008, January and June  
 366 2009 respectively,  $p < 0.01$ ). TA concentrations appeared to be always significantly and  
 367 positively correlated to salinity (or water height) ( $R$ : 0.93 and 0.80,  $p < 0.01$  in September 2008  
 368 and April 2009 for instance) and to DIC concentrations (Figs. 2, 3).  $\delta^{13}\text{C}$ -DIC values were  
 369 significantly and positively correlated to salinity and water height (H) values in July 2008 and  
 370 over all 2019 cycles ( $R$ : 0.45, 0.70 in July 2008 and April 2009 respectively,  $p < 0.01$ ), to TA  
 371 values in September 2008 and over all cycles in 2019 ( $R$ : 0.46, 0.59 in September 2008 and  
 372 2009 respectively,  $p < 0.01$ ) and to DIC concentrations over all cycles in 2009 ( $R$ : 0.61 and 0.76  
 373 in April and June 2009 respectively) (Fig. 4).

### 3.2. Gas transfer velocities and atmospheric CO<sub>2</sub> fluxes from the Arcachon lagoon waters

Wind speeds ( $U_{10}$ ) ranged between  $2.41 \pm 1.05$  and  $7.74 \pm 1.77$  m s<sup>-1</sup> in September and November 2008 respectively with significant differences noticed between September 2008 - January 2009 (minimum values) and July - November 2008 - September 2009 (maximum values) (Kruskal-Wallis and Dunn's post-test,  $p < 0.01$ , Table 2).  $k_{600}$  values were in average estimated at  $8.54 \pm 6.75$ ,  $17.29 \pm 15.76$  and  $17.00 \pm 6.23$  cm h<sup>-1</sup> according to W92, RC01 and A09 equations respectively (see Material and Methods, Table 2). Minimum mean values occurred in September 2008 - January 2009 ( $1.82 \pm 1.25$ ,  $4.4 \pm 1.36$  and  $9.58 \pm 3.3$  cm h<sup>-1</sup> in January 2009 with the three methods respectively, Table 2) whereas the highest values were reached in November 2008 - September 2009 ( $19.37 \pm 8.37$ ,  $33.33 \pm 19.51$  and  $28.38 \pm 6.12$  cm h<sup>-1</sup> in November 2008 with the three methods respectively, Table 2). In April 2008 and September 2009 at high tide,  $k_{600}$  (and  $U_{10}$ ) values were also found significantly different between day (higher values) and night (lower values) periods (Mann-Whitney test,  $p < 0.05$ ) whatever used methods (Table 2).

Mean water-air CO<sub>2</sub> fluxes were estimated at  $0.27 \pm 0.22$ ,  $0.56 \pm 0.54$  and  $0.55 \pm 0.22$  mmol m<sup>-2</sup> h<sup>-1</sup> according to W92, RC01 and A09 equations respectively (Table 2). Minimum mean values were observed in January 2009 ( $0.06 \pm 0.04$ ,  $0.14 \pm 0.06$  and  $0.29 \pm 0.13$  mmol m<sup>-2</sup> h<sup>-1</sup> with the three methods respectively) whereas the highest values were reached in September 2009 ( $0.62 \pm 0.66$ ,  $1.67 \pm 2.36$  and  $0.82 \pm 0.47$  mmol m<sup>-2</sup> h<sup>-1</sup> with the three methods respectively, Table 2). In April 2008 and September 2009, water-air CO<sub>2</sub> flux values were also found significantly different between day (higher values) and night (lower values) periods (Mann-Whitney test,  $p < 0.05$ ) as it was the case for  $k_{600}$  and  $U_{10}$  values whatever used methods (Table 2). Water-air fluxes estimated from A09 equation were significantly higher than values estimated from W92 (and RC01) equations (Kruskal-Wallis and Dunn's post-test,  $p < 0.01$ )

except in November 2008 - April 2009 - September 2009 where no significant difference was observed between methods.

In July 2008, an atmospheric EC mast was deployed in the Arcachon lagoon simultaneously and close (at 1.8 km) to the 24 hours cycle location (Fig. 1, Table 2; Polsenaere et al. 2012a). During the whole tidal cycle in July 2008, EC fluxes averaged  $0.45 \pm 7.71 \text{ mmol m}^{-2} \text{ h}^{-1}$  and ranged from -17.98 to 43.19  $\text{mmol m}^{-2} \text{ h}^{-1}$ . EC water-air  $\text{CO}_2$  fluxes during the immersion were on average  $-1.39 \pm 2.67 \text{ mmol m}^{-2} \text{ h}^{-1}$  and ranged from -12.38 to 2.10  $\text{mmol m}^{-2} \text{ h}^{-1}$  with significantly lower values during daytime period (Mann-Whitney test,  $p < 0.05$ ). Significant differences were computed between direct water-air  $\text{CO}_2$  fluxes measured during the immersion at the EC site and calculated  $\text{CO}_2$  fluxes from  $\text{pCO}_2$  records at the channel site according to RC01 - A09 equations (Kruskal-Wallis and Dunn's post-test,  $p < 0.01$ ; Table 2).

## **4. Discussion**

### **4.1. Seasonal compensation of thermal and non-thermal effects on water $\text{pCO}_2$**

In the Arcachon lagoon, seasonal variations in water inorganic carbon parameters and especially  $\text{pCO}_2$  were relatively weak and on the lower range for waters influenced by an intertidal ecosystem when compared to other coastal ecosystems worldwide (Borges et al. 2005; Table 3). We observed a maximal  $\text{pCO}_2$  variation of 196 ppmv between the lowest and the highest values measured during each 12- or 24-hour cycles and the maximum  $\text{pCO}_2$  (averaged over each 24-hour cycle) amplitude barely reached 70 ppmv.

At the seasonal scale over coastal bays, thermal but also non-thermal effects can significantly influence water  $\text{pCO}_2$  variations. In the studied lagoon, we observed that, seasonally, biological effects that consisted in more heterotrophy in winter and more autotrophy in summer, was offset by the thermal effect induced by the variation of water temperature (from 8.9 to 22.2 °C) resulting in relatively constant  $\text{pCO}_2$  values throughout the year. Furthermore, other non-

thermal effects were induced by mixing of freshwater in the lagoon, particularly in January 2009 when salinity decreased down to 20.4 (Table 1, Figs. 3, 4). River waters discharging in the lagoon are yearly oversaturated in CO<sub>2</sub> (Polsenaere et al. 2012b) and their positive influence on pCO<sub>2</sub> values was supposed to be maximal in January 2009 (Table 1, Fig. 3). Overall, thermal and non-thermal components of pCO<sub>2</sub> strongly varied seasonally, almost compensating each other. For instance, the six months  $\Delta$ TpCO<sub>2</sub> offset (260 ppmv) observed from July 2008 to January 2009 (TpCO<sub>2</sub> from 601 to 341 ppmv) concomitantly to the 13.3 °C water temperature decrease (from 22.2 to 8.9 °C) barely compensated non-thermal effects on water pCO<sub>2</sub> that occurred during that six-month period ( $\Delta$ NpCO<sub>2</sub> = 317 ppmv, from 381 to 698 ppmv) (Fig. 2). In spring and summer, more autotrophic metabolism by all benthic and planktonic primary producers of the lagoon is favored and less remineralization occurs resulting in the lowest NpCO<sub>2</sub> values, while the effect of autotrophy on pCO<sub>2</sub> is offset by water heating. Phytoplankton blooms occur in the lagoon especially from the spring season that shows the highest primary production rates (between 231.4 and 496.6 mg C m<sup>-3</sup> d<sup>-1</sup> in 2003, Glé et al. 2008). Influxes of CO<sub>2</sub> in spring and early autumn were measured on the flat by the EC station (Polsenaere et al. 2012a). *Zostera* seagrass meadows also contribute significantly to the total primary production of the Bay (Plus et al. 2015; Polsenaere et al. 2012a; Ribaud et al. 2017) and then may influence pCO<sub>2</sub> dynamics as observed elsewhere in the eastern shore of Virginia by Berg et al. (2019). In summer in the lagoon, higher *Zostera* seagrass net primary production associated with lower heterotrophic respiration result in more autotrophic sediment metabolism; together with phytoplanktonic and immersed *Zostera* production and lower freshwater inputs to the lagoon explain the NpCO<sub>2</sub> drawdown from January to June 2009 (281, from 698 to 417 ppmv). However, in summer, *Zostera* primary production probably occurs using mostly CO<sub>2</sub> directly from the atmosphere during the emersion and even more if low tide is around midday (Polsenaere et al. 2012a). Thus, in the studied channel the direct influence of *Zostera*

metabolism on water  $p\text{CO}_2$  is probably modest. To the contrary from spring to summer-autumn 2009 periods,  $\text{NpCO}_2$  values increased (46, from 417 to 463 ppmv) whereas primary production decreased. In autumn and winter contrarily to summer season, heterotrophy is favored because the seagrass biomass is recycled and decomposed in the sediments and the waters (Auby and Labourg 1996). The *Zostera* meadow decline feeds the lagoon sediments and waters with organic matter, favoring heterotrophy which together with a lower planktonic primary production and also more freshwater inputs to the lagoon, contribute to the highest  $\text{NpCO}_2$  values measured in November 2008 and January 2009 (Fig. 2). At the same time, this combination of all factors on water  $p\text{CO}_2$  is compensated by water cooling and in consequence, a  $p\text{CO}_2$  value seasonally constant at about 500 ppmv was measured in the lagoon. Other studies showed a more pronounced effect of either thermal or non-thermal variations on water  $p\text{CO}_2$  at the seasonal scale as for instance Ribas-Ribas et al. (2011) that reported in the Bay of Cadiz during winter a dominant thermal control in comparison with non-thermal effects, or to the contrary, Bozec et al. (2011) who showed in the Bay of Brest, a stronger influence of non-thermal (biology) processes on seasonal  $p\text{CO}_2$  dynamics (Table 3).

#### **4.2. Seasonal carbonate chemistry and mixing patterns of freshwater and seawater DIC**

Besides biological activity and its light-temperature controlled seasonal evolution, horizontal advection and exchanges between terrestrial-lagoon-oceanic waters producing different mixing patterns, strongly drives observed carbonate chemistry at the seasonal scale in the lagoon. Hydrodynamic forcing importance was shown in other tidal systems such as a freshwater or salty marshes where intense exchanges between marsh and coastal/estuarine waters occurred during hydrological floods (Neubauer and Anderson 2003, and references in Table 3). Intense exchanges of oceanic and continental waters occurred within the Arcachon lagoon as well through channels or over the tidal flat around high tide (Plus et al. 2009; Polsenaere et al. 2012a,

473 b). A significant influence of freshwater discharge in the lagoon occurred in winter of the year  
474 2009 with the lowest salinities (20.5-24.5) associated to the lowest TA concentrations (1.493-  
475 1.733 mmol kg<sup>-1</sup>) measured through our tidal cycle sampling (Fig. 3e). These low values  
476 especially at low tide reflected the freshwater inputs to the lagoon from rivers draining the  
477 podzolized acidic catchment (Polsenaere et al. 2012b). Furthermore, in the lagoon, water  
478 seasonal mean TA values were always above corresponding DIC concentrations (maximum  
479 hourly measured DIC values were below minimum TA values too) except in January and April  
480 2009. It highlights the seawater influence at the sampled channel station in the middle position  
481 inside the lagoon where CO<sub>3</sub><sup>2-</sup> provides the first line of buffering capacity as observed by Wang  
482 et al. (2016) in the Sage Lot Pond salt marsh system. The significant positive correlations  
483 between δ<sup>13</sup>C-DIC values and salinity values, TA values and DIC concentrations over all 2019  
484 cycles (Fig. 4a, c, d) supports the importance of alkalinity (CO<sub>3</sub><sup>2-</sup>) among other DIC species  
485 and thus an overall seasonal DIC variation control through tidal forcing.

486 Comparing apparent 0 end-member TA and *in situ* catchment TA values at each cycle (season),  
487 we highlighted that alkalinity production occurred within the lagoon especially in April, July  
488 2008 and September 2009 when 0 end-member TA values were at least two times higher than  
489 *in situ* catchment weighted mean TA values (Fig. 4b). The Arcachon flat constitutes an  
490 important stock of carbonates of about 120 Mt of several shellfish species represented at 95 %  
491 by *Crassostrea gigas* (Polsenaere et al. 2012a). From the end of the reproduction season  
492 (November) to the spat removing in spring, early development stages of bivalves are  
493 particularly sensitive to dissolution-induced mortalities as shown by Barros et al. (2013)  
494 through larval viability laboratory experiments on the Pacific oyster *Crassostrea gigas*. Thus,  
495 CaCO<sub>3</sub> dissolution could occur in wet mud sediments in presence of such shellfishes patchily  
496 distributed on the tidal flat. To the contrary, in late summer (September) and autumn  
497 (November) 2008, *in situ* catchment TA values were slightly higher than 0 end-member TA

values supporting the possibility of calcification processes in the lagoon (Fig. 4b). Seagrass systems are recognized to be important site of high calcium carbonate ( $\text{CaCO}_3$ ) cycling, both in terms of production and dissolution, such as *Posidonia oceanica* meadows where  $\text{CaCO}_3$  precipitation can overwhelm sediment  $\text{CaCO}_3$  dissolution particularly during net autotrophic periods (Barron et al. 2006). In any cases, net TA production in the lagoon remains more important in comparison with calcification at the annual scale.

#### **4.3. Processes controlling tidal and diurnal $\text{pCO}_2$ and DIC variations**

##### ***4.3.1. Large tidal DIC variations through current advection***

Over intertidal systems as Arcachon, horizontal advection can strongly control water  $\text{pCO}_2$  and carbonate chemistry variations at the tidal scale too. Significant negative correlations between  $\text{pCO}_2$  and salinity or water height occurred most of the time in each season (except in Sept. and Nov. 08) and for each tidal/diurnal periods. The fact that higher  $\text{pCO}_2$  values associated to lower salinity and depth values at low tide (opposite pattern during high tide) were systematically measured irrespective of day or night status supports the significant tidal rhythm control on water  $\text{pCO}_2$  in the lagoon. For example, during the June 2009 cycle,  $\text{pCO}_2$  and TA values were significantly inversely correlated and respectively negatively and positively correlated to water height, salinity and  $\delta^{13}\text{C}$ -DIC values. Significantly higher TA concentrations associated to higher  $\delta^{13}\text{C}$ -DIC values (typical oceanic TA and  $\delta^{13}\text{C}$ -DIC values) were also measured during high tide periods contrarily to  $\text{pCO}_2$  values (Table 1, Fig. 3). These results clearly reflected tidal forcing on carbonate chemistry through ocean exchange with more buffered waters on one hand and riverine inputs with more acidic waters on the other hand. In the Arcachon lagoon, maximum  $\text{pCO}_2$  values measured at low tide were well below those measured over other coastal systems as tidal flats nearby and small marsh-estuary or mangrove tidal creeks further (Table 3). A 24 hour-cycle performed in May 2006 (not shown) in a shallower creek close to the outlet

of a small river North East in the back of the Arcachon lagoon showed the highest  $p\text{CO}_2$  values (up to 1300 ppmv, salinity values close to 28) at mid-ebb when the tidal flat was still immersed compared to the low tide period, when the flat was emerged and the channel connected to the river, with associated decreased and lower  $p\text{CO}_2$  and salinity values (close to 800 ppmv and 22-23, respectively, data not shown). Thus, these measurements suggest another associated process (i.e. tidal pumping, see next 4.3.2. discussion part) along with freshwater mixing that occur together in the Arcachon flat.

#### ***4.3.2. Tidal porewater pumping and associated water alkalinity production and $p\text{CO}_2$ variations***

During tidal cycles conducted at the channel station, TA (or DIC) concentrations showed overall weak tidal variations (Fig. 3). Porewater pumping over tidal coastal vegetated ecosystems (seagrass meadows, salt marshes and mangroves) has been recognized as an important process in water DIC production (Neubauer and Anderson 2003; Wang et al. 2016; Borges et al. 2003; Maher et al. 2013). Indeed, high alkalinity values can be reached through aerobic respiration coupled to carbonate dissolution but also through organic matter anaerobic remineralization products, i.e.  $\text{N}_2$  from net denitrification and reduced sulfur (pyrite burial) from net sulfate reduction (Hu and Cai 2011). In Arcachon, tidal pumping has been highlighted as a significant process controlling benthic phosphorus and iron cycles over seagrasses where below the rhizosphere, Fe(II) can be exposed to a reduced environment and precipitates as FeS and pyrite (Deborde et al. 2008b). De Wit (2008) showed the importance of sulfate-reducing bacteria in *Zostera* seagrass sediments at a tidal flat station very close to our 24-hour cycle station. Moreover, Heijs et al. (1999) showed at the same location that a substantial population of aerobic sulfide-oxidizing bacteria was also present, buffering free sulfide through chemical processes with iron leading to high FeS and pyrite concentrations in sediments. In particular,



sulfide oxidation (depending on whether sulfide will be oxidized to sulfate or to sulfur) was estimated at  $4694 \times 10^3$  or  $1174 \times 10^3 \text{ mol cm}^{-3} \text{ day}^{-1}$ , whereas previously measured sulfate reduction rates at the same station ranged from 150 to  $1300 \text{ nmol cm}^{-3} \text{ day}^{-1}$ . These findings along with the quantitative apparent 0 end-member and *in situ* catchment TA value (Fig. 4b) suggest a substantial TA production through tidal porewater pumping along the year. Its influence on TA (or DIC) production in the lagoon could not be clearly seen from our chosen site, which have high salinities and TA values, hiding the terrestrial influence and did not cover the 0 end-member. In any cases, in Arcachon, alkalinity production through tidal pumping is not so strong in comparison with other mentioned mangrove or saltmarsh systems. Maher et al. (2013) measured in a small tidal mangrove creek (Australia) during summer and winter a clear tidal trend for DIC as in the present study (highest and lowest values reached during low and high tides, respectively). However, a  $0.736 \text{ mmol kg}^{-1}$  DIC range (between 2.064 and  $2.8 \text{ mmol kg}^{-1}$ ) was measured there when in the Arcachon channel we only measured a tidal DIC variation of  $0.216 \text{ mmol kg}^{-1}$  (April 2009) at maximum ( $0.116 \text{ mmol kg}^{-1}$  in average over the whole study period). In the Sage Lot Pond tidal marsh, Wang et al. (2016) measured in Summer tidal TA variation ranges close to  $0.4 \text{ mmol kg}^{-1}$  respectively when at Arcachon a variation of  $0.261 \text{ mmol kg}^{-1}$  at maximum ( $0.133 \text{ mmol kg}^{-1}$  in average) was seen. Similarly, according to tidal  $\text{pCO}_2$  variations, smaller variations were measured in comparison to other salt marsh-estuary or mangrove creek systems, where stronger tidal  $\text{pCO}_2$  variations were observed according to porewater mixing (Table 3).

#### ***4.3.3 Significant diurnal $\text{pCO}_2$ patterns linked to biological activity***

In subtidal coastal ecosystems, pelagic and benthic biological activities can generate large diurnal water  $\text{pCO}_2$  variations. Indeed, in comparison with Arcachon, similar and even higher diurnal  $\text{pCO}_2$  ranges were measured in macrophyte meadows (Baltic Sea, Florida and Virginia)

or in bay channels (Spain) (Table 3). However, in these subtidal ecosystems, tidal pumping was supposed to be minor; in the Arcachon lagoon, pCO<sub>2</sub> variations occur at the tidal scale through porewater pumping and water masses mixing, these latter being superposed on those occurring at the diurnal scale and linked to solar radiation and light availability.

During all sampled cycles, no significant pCO<sub>2</sub> versus Chl-*a* concentration relationships were computed and Chl-*a* concentrations never reached more than 1.9 µg L<sup>-1</sup> in average (data not shown). Our successive tidal/diurnal cycle samplings in the central lagoon channel were apparently not able to fully catch these blooms especially in spring and summer. However, interesting diurnal pCO<sub>2</sub> patterns related to biological activity could be detected when comparing nighttime with daytime values for a same salinity range. For instance, in September 2008, at low tide in the channel for a salinity range values close to 33, lower water pCO<sub>2</sub> and higher temperature values were measured at daytime (400-525 ppmv, > 20 °C) than at nighttime (550-600 ppmv, close to 19 °C) (Fig. 5e, f). The same pattern was observed in June 2009 as well (Fig. 5m, n). Phytoplankton possibly with resuspended microphytobenthos communities in the channel then appeared to be active at that moment. Savelli et al. (2019) showed precisely that almost half (43 %) of MPB primary production can be resuspended annually over intertidal lagoons and the highest occurs in spring tide at the flood beginning due to high current velocities and low water heights. To the contrary, in April 2009 during flooding, water pCO<sub>2</sub> (500-560 ppmv) increased (while S increased and T decreased) whereas during ebbing, water pCO<sub>2</sub> (538-494 ppmv) decreased and was lower (while S decreased and T increased) (Fig. 5k, l). At that particular moment in the channel, organic matter produced by primary production could feed community respiration through incoming coastal waters during flooding. The significant negative correlation computed between pCO<sub>2</sub> and δ<sup>13</sup>C-DIC values is consistent with an organic matter mineralization process that occurred in spring in the lagoon.

To assess the biological control on measured  $p\text{CO}_2$  patterns in the studied channel, we statistically compared, when possible, night and day  $p\text{CO}_2$  values averaged over the same salinity range (i.e. with no significant salinity value difference between day and night periods) according to tide phases for each cycle (Table 4). During flooding, daytime  $p\text{CO}_2$  were significantly lower than those nighttime  $p\text{CO}_2$  values and to the contrary, during ebbing phase, daytime  $p\text{CO}_2$  were significantly higher night time  $p\text{CO}_2$  values. At the same time, significant variations in water temperature between day and night times for both flooding and ebbing periods occurred. Water temperature gradients exist and could influence diurnal  $p\text{CO}_2$  variations. However, they cannot alone explain these variations at our sampling station since differences between the theoretical  $p\text{CO}_2$  variations due to diel temperature differences and measured changes in water  $p\text{CO}_2$  for the same salinity range are large (Table 4).

Overall, these reproducible patterns strongly support the control of  $p\text{CO}_2$  by biological activity (primary production of phytoplankton, MPB and seagrasses). Koné et al. (2009) reported  $p\text{CO}_2$ -oversaturated waters in some lagoons of Ivory Coast (West Africa) behaving as macrotidal estuaries due to net ecosystem heterotrophy and riverine  $\text{CO}_2$  rich water inputs. To the contrary  $p\text{CO}_2$ -undersaturated waters were found in the other lagoons showing permanent hyaline stratification leading to higher phytoplankton biomass. In other systems such as Tampa and Florida bays,  $p\text{CO}_2$  diurnal variability was mostly influenced by biological processes such as photosynthesis/respiration of benthic communities and precipitation/dissolution of calcium carbonate respectively (Table 3). Interestingly and contrary to other studied salt marsh and mangrove systems (Table 3) where tidal pumping is predominant, water  $p\text{CO}_2$  and DIC variations in the Arcachon lagoon seemed to result from the subtle combination of thermal, water column primary production, and tidal pumping effects along with thermodynamic mixing between seawater and freshwater.

#### 4.4. High heterogeneity in water-air CO<sub>2</sub> fluxes over the Arcachon lagoon

##### *4.4.1. Turbulence forcing control on water-air CO<sub>2</sub> flux temporal variability*

The subsurface waters of the Arcachon lagoon remained always oversaturated and close to the atmospheric equilibrium at both seasonal and diurnal scales. Annual mean air-sea CO<sub>2</sub> fluxes were estimated at  $0.27 \pm 0.22$ ,  $0.56 \pm 0.54$  and  $0.55 \pm 0.22$  mmol m<sup>-2</sup> h<sup>-1</sup> depending on the gas transfer velocity-wind parameterizations. Water-air CO<sub>2</sub> flux values remained in the lower range of annual values reported for macrotidal estuaries ( $0.58$ - $8.42$  mmol m<sup>-2</sup> h<sup>-1</sup>) (Borges et al. 2005). Similar intertidal systems showed different values with more variations at both diurnal and seasonal scales (Table 3). In other subtidal and marine systems, fluctuations between CO<sub>2</sub> sink and source could also be measured over the year depending on seasons (Table 3).

In the Arcachon lagoon, wind speed influence on calculated air-sea CO<sub>2</sub> fluxes was significant and could be more important in determining the intensity of the flux, than the pCO<sub>2</sub> air-sea gradient itself. Despite significant pCO<sub>2</sub> variations generally noticed at seasonal and tidal/diurnal scales, only few significant air-sea CO<sub>2</sub> flux differences were observed (i.e. between November and September 2008 and between September 2008 and 2009), concomitantly to significant differences in U<sub>10</sub> and K<sub>600</sub> values (Table 2). Thus, air-sea CO<sub>2</sub> flux variability in the Arcachon lagoon at all temporal scales appears to be controlled by turbulence (K<sub>600</sub>, physical forcing) rather than air-water pCO<sub>2</sub> gradients. This finding is the opposite of what it is generally observed over dynamic coastal bays at temperate and tropical latitudes characterized by higher diurnal/tidal water pCO<sub>2</sub> gradients (Table 3).

##### *4.4.2. High heterogeneity in water-air CO<sub>2</sub> fluxes according to space and methodology*

CO<sub>2</sub> fluxes were estimated at the water-air interface based on k<sub>600</sub> parameterizations from Wanninkhof et al. (1992), Raymond and Cole (2001) and Abril et al. (2009). These parameterizations were obtained over oceanic and estuarine systems with different approaches,

i.e. the bomb  $^{14}\text{C}$  inventory in the ocean, non-intrusive tracer data and chamber measurements respectively. The Abril et al. (2009) relationship gave significantly higher flux values compared to the two others, potentially due to bottom current contributions from 2 to 20 cm  $\text{s}^{-1}$  according to seasons and associated hydrodynamic modelling estimations. In July of the year 2008, significant differences were computed between simultaneous direct EC fluxes and estimated fluxes from gas transfer parameterizations (Table 2). No  $k_{600}$  calculations or flux data comparisons were attempted from these simultaneous EC flux and water  $\text{pCO}_2$  measurements due to strong spatial heterogeneity in water bodies (separated from 1.8 km) highlighted in the present study and due to the strong variability in gas transfer velocity and  $\text{CO}_2$  flux calculations according to methodologies too (Polsenaere et al. 2012a; Raymond and Cole 2001; Vachon et al. 2010).

Indeed, variability in water  $\text{pCO}_2$  and air-sea  $\text{CO}_2$  fluxes depends on site locations inside a same coastal ecosystem at the different temporal scales. The spring 2006 cycle carried out in the back of the Arcachon lagoon (4.3.1. discussion part) showed higher water  $\text{pCO}_2$  tidal variations (680-1330 ppmv) and resulted in a higher  $\text{CO}_2$  source to the atmosphere at this more terrestrial influenced location. These observations suggest that large differences in water  $\text{pCO}_2$  and sea-air  $\text{CO}_2$  fluxes could occur at smaller spatial scale due to specific processes and characteristics that exist at the sampled area. In the lagoon, benthic primary producers such as *Zostera noltei* seagrass meadows and resuspended microphytobenthic communities could influence in a different way carbon dynamics and air-sea fluxes at the channel station sampled here, compared to swallow waters above the tidal flat as revealed by EC measurements (Polsenaere et al. 2012a). Indeed, a  $\text{CO}_2$  influx was detected during the emersion by the EC, but we never observed  $\text{CO}_2$  undersaturated waters in the channel during the July 2008 cycle. Due to the strong influence of tidal advection on water  $\text{pCO}_2$  in the intertidal lagoon, water masses sampled at the studied station were not the same as those caught in the EC footprint during in July 2008

(Tables 1 and 2, Polsenaere et al. 2012a). This could also explain the significant differences in air-sea CO<sub>2</sub> fluxes and associated gas transfer velocities we got from both methodologies, and methodological and logistical complexity to get concomitant water-air EC flux and equilibrator water pCO<sub>2</sub> values from the same water mass in the lagoon. Wang et al. (2018) over the Duplin River salt marsh-estuary (Georgia), though different from Arcachon due to the most of the time emersion canopy (ecosystem-atmosphere flux there versus water-atmosphere flux based on water pCO<sub>2</sub> here) specifically suggested EC measurements of salt marsh net ecosystem exchange could underestimate net ecosystem production for not accounting for lateral DIC exchanges with tidal inundation.

## **Conclusions**

Waters of the Arcachon lagoon represents a permanent weak CO<sub>2</sub> supersaturation characterized by a seasonal compensation of thermal and biological effects and carbonate chemistry and mixing patterns of freshwater and seawater DIC. At smaller time scales if large tidal DIC variations through current advection were observed, weak tidal porewater pumping and associated water alkalinity production and pCO<sub>2</sub> variations were noticed compared to other tidal creeks surrounded by mangrove or saltmarshes. Accurate water monitoring such as that carried out in this study permits high resolution analysis of the carbon signal; small but significant pCO<sub>2</sub> variations were seen at the diurnal scale (between 5 and 24 ppmv) linked to the light cycle apparently induced by planktonic and benthic productivity in the channel along to day versus night temperature gradients at flooding and ebbing periods. The temporal variability and the high heterogeneity in computed water-air CO<sub>2</sub> fluxes according to space (water masses) and methodology (EC, ...) would require more integrated carbon fluxes and processes over tidal ecosystems as here for the Arcachon lagoon.

## Acknowledgments

We would like to express our thanks to Francis Prince the Planula boat captain. This paper is a contribution to the PNEC (Programme National Environnement Côtier)-Littoral Atlantique and ANR PROTIDAL (Agence Nationale de la Recherche « Processus biogéochimiques transitoires de la zone intertidale ») projects.

## Competing Interests

The authors declare no competing interests.

## References

- Abril, G., M. Commarieu, A. Sottolichio, P. Bretel, and F. Guérin. 2009. Turbidity limits gas exchange in a large macrotidal estuary. *Estuarine, Coastal and Shelf Science* 83: 342–348.
- Abril, G., Deborde, J., Savoye, N., Mathieu, F., Moreira-Turcq, P., Artigas, F., Meziane, T., Takiyama, L. R., de Souza, M. S., Seyler, P. 2013. Export of  $^{13}\text{C}$ -depleted dissolved inorganic carbon from a tidal forest bordering the Amazon estuary. *Estuarine, Coastal and Shelf Science*, 129: 23-27.
- Amanieu, M. 1967. Recherches écologiques sur la faune des plages abritées et des étangs saumâtres de la région d’Arcachon. *PhD Thesis, Université Bordeaux I*, pp. 234.
- Amorocho, J. and J.J. DeVries. 1980. A new evaluation of the wind stress coefficient over water surfaces. *Journal of Geophysical Research* 85: 433–442.
- Auby, I., F. Manaud, D. Maurer, and G. Trut. 1994. Étude de la prolifération des algues vertes dans le bassin d’Arcachon. *Report Prepared by IFREMER, Arcachon, France, for CEMAGREF-SSA-SABARC*, pp. 1–163.

721 Auby, I. and P.J. Labourg. 1996. Seasonal dynamics of *Zostera noltii* Hornem. in Bay of  
 722 Arcachon (France). *Journal of Sea Research* 35: 269–277.

723 Barron, C., C. M. Duarte, M. Frankignoulle, and A.V. Borges. 2006. Organic carbon  
 724 metabolism and carbonate dynamics in a Mediterranean seagrass (*Posidonia oceanica*)  
 725 meadow. *Estuaries and Coasts* 29: 417–426.

726 Barros, P., P. Sobral, P. Range, L. Chícharo, and D. Matias. 2013. Effects of sea-water  
 727 acidification on fertilization and larval development of the oyster *Crassostrea gigas*.  
 728 *Journal of Experimental Marine Biology and Ecology* 440: 200–206.  
 729 <https://doi.org/10.1016/j.jembe.2012.12.014>.

730 Bauer, J.E., W.-J. Cai, P.A. Raymond, T.S. Bianchi, C.S. Hopkinson, and P.A.G. Regnier.  
 731 2013. The changing carbon cycle of the coastal ocean. *Nature* 504 (7478): 61–70.

732 Berg, P., M.L. Delgard, P. Polsenaere, K.J. McGlathery, S.C. Doney S.C., and A.C. Berger.  
 733 2019. Dynamics of benthic metabolism, O<sub>2</sub>, and pCO<sub>2</sub> in a temperate seagrass meadow.  
 734 *Limnology and Oceanography* 64: 2586–2604.

735 Borges, A.V. and M. Frankignoulle. 1999. Daily and seasonal variations of the partial pressure  
 736 of CO<sub>2</sub> in surface seawater along Belgian and southern Dutch coastal areas. *Journal of*  
 737 *Marine Systems* 19 (4): 251–266.

738 Borges, A. V., S. Djenidi, G. Lacroix, J. Théate, B. Delille, and M. Frankignoulle. 2003.  
 739 Atmospheric CO<sub>2</sub> flux from mangrove surrounding waters. *Geophysical Research Letters*  
 740 30(11), 1558. <https://doi.org/10.1029/2003GL017143>.

741 Borges, A. V., B. Delille, and M. Frankignoulle. 2005. Budgeting sinks and sources of CO<sub>2</sub> in  
 742 the coastal ocean: diversity of ecosystems counts. *Geophysical Research Letters* 32:  
 743 LI4601. <https://doi:10.1029/2005GL023053>.



744 Borges, A.V. and G. Abril. 2011. Carbon dioxide and methane dynamics in estuaries.  
 745 In *Treatise on estuarine and coastal science*, ed. E. Wolanski and D.S. McLusky 5: 119–  
 746 161.

747 Bouillon, S., Middelburg, J.J., Dehairs, F., Borges, A.V., Abril, G., Flindt, M.R., Ulomi, S.,  
 748 Kristensen, E. 2007. Importance of intertidal sediment processes and porewater exchange  
 749 on the water column biogeochemistry in a pristine mangrove creek (Ras Dege, Tanzania).  
 750 *Biogeosciences* 4 (3): 311–322.

751 Bozec, Y., L. Merlivat, A.-C. Baudoux, L. Beaumont, S. Blain, E. Bucciarelli, T. Danguy, E.  
 752 Grossteffan, A. Guillot, and J. Guillou. 2011. Diurnal to inter-annual dynamics of pCO<sub>2</sub>  
 753 recorded by a CARIOCA sensor in a temperate coastal ecosystem (2003–2009). *Marine*  
 754 *Chemistry* 126: 13–26.

755 Burgos, M., T. Ortega, and J. Forja. 2018. Carbon Dioxide and Methane Dynamics in Three  
 756 Coastal Systems of Cadiz Bay (SW Spain). *Estuaries and Coasts* 41: 1069–1088.  
 757 <https://doi.org/10.1007/s12237-017-0330-2>.

758 Cai, W.J., L.R. Pomeroy, M.A. Moran, and Y. Wang. 1999. Oxygen and carbon dioxide mass  
 759 balance for the estuarine-intertidal marsh complex of five rivers in the southeastern US.  
 760 *Limnology and Oceanography* 44: 639–649.

761 Cai, W.-J. 2011. Estuarine and coastal ocean carbon paradox: CO<sub>2</sub> sinks or sites of terrestrial  
 762 carbon incineration? *Annual Review of Marine Science* 3 (1): 123–145.

763 Canton, M, P. Anschutz, A. Coynel, P. Polsenaere, I. Auby, and D. Poirier. 2012. Nutrient  
 764 export to an Eastern Atlantic coastal zone: first modeling and nitrogen mass balance.  
 765 *Biogeochemistry* 107: 361–377.

766 Caumette, P., J. Castel, and Herbert R. 1996. Coastal Lagoon Eutrophication and ANaerobic  
 767 Processes (C.L.E.AN.): Nitrogen and Sulfur Cycles and Population Dynamics in Coastal

768 Lagoons. *A Research Programme of the Environment Programme of the EC (DG XII)*.  
769 <https://doi.org/10.1007/978-94-009-1744-6>.

770 Chen, C.-T.A., Huang, T.-H., Chen, Y.-C., Bai, Y., He, X., Kang, Y. 2013. Air–sea exchanges  
771 of CO<sub>2</sub> in the world’s coastal seas. *Biogeosciences* 10, 6509–6544.  
772 <https://doi.org/10.5194/bg-10-6509-2013>.

773 Cognat, M., F. Ganthy, I. Auby, F. Barraquand, L. Rigouin, and A. Sottolichio,  
774 2018. Environmental factors controlling biomass development of seagrass meadows of  
775 *Zostera noltei* after a drastic decline (Arcachon Bay, France). *Journal Of Sea Research*  
776 140: 87–104.

777 Coignot, E., P. Polsenaere, P. Soletchnik, O. Le Moine, P. Souchu, E. Joyeux, Y. Le Roy, J.-P.  
778 Guéret, L. Froud, R. Gallais, E. Chourré, and L. Chaigneau. 2020. Variabilité spatio-  
779 temporelle des nutriments et du carbone et flux associés le long d’un continuum terrestre-  
780 aquatique tempéré (Marais poitevin – Baie de l’Aiguillon – Pertuis Breton). Rapport final  
781 (suivi 2017-2018) - Projet Aiguillon (2016-2020).  
782 111pp. <https://archimer.ifremer.fr/doc/00618/73003/>

783 Cole, J.J., Y.T. Prairie, N.F. Caraco, W.H. McDowell, L.J. Tranvik, R.G. Striegl, C.M. Duarte,  
784 P. Kortelainen, J.A. Downing, J. Middleburg, and J. Melack. 2007. Plumbing the global  
785 carbon cycle: integrating inland waters into the terrestrial carbon budget. *Ecosystems* 10:  
786 171–184.

787 Cotovicz, L.C., B.A. Knoppers, N. Brandini, S.J. Costa Santos, and G. Abril. 2015. A large  
788 CO<sub>2</sub> sink enhanced by eutrophication in a tropical coastal embayment (Guanabara Bay,  
789 Rio de Janeiro, Brazil). *Biogeosciences* 12: 6125–6146. [https://doi.org/10.5194/bg-12-](https://doi.org/10.5194/bg-12-6125-2015)  
790 6125-2015.

791 Cotovicz, L.C., B.G. Libardoni, N. Brandini, B.A. Knoppers and G. Abril. 2016. Comparações  
792 entre medições em tempo real da pCO<sub>2</sub> aquática com estimativas indiretas em dois

793        estuários tropicais contrastantes: o estuário eutrofizado da baía de Guanabara (RJ) e o  
794        estuário oligotrófico do rio São Francisco (AL). *Química Nova*. 39: 1206–1214.  
795        <https://doi.org/10.21577/0100-4042.20160145>.

796    Dai, M., Z. Lu, W. Zhai, B. Chen, Z. Cao, K. Zhou, W. J. Cai, and C. T. A. Chen. 2009. Diurnal  
797        variations of surface seawater pCO<sub>2</sub> in contrasting coastal environments. *Limnology and*  
798        *Oceanography* 54: 735–745.

799    Deborde, J., P. Anschütz, I. Auby, C. Glé, M.V. Commarieu, D. Maurer, P. Lecroart, G. Abril.  
800        2008a. Role of the tidal pumping on nutrient cycling in a temperate lagoon (Arcachon  
801        Bay, France). *Marine Chemistry* 109: 98–114.

802    Deborde J., G. Abril, A. Mouret, D. Jezequel, G. Thouzeau, J. Clavier, G.  
803        Bachelet, P. Anschütz. 2008b. Impacts of seasonal dynamics impact of a *Zostera*  
804        *noltii* meadow on phosphorus and iron cycles in a tidal mudflat (Arcachon Bay,  
805        France), *Marine Ecology Progress Series* 355, 59–71.

806    Delgard, M. L., B. Deflandre, J. Deborde, M. Richard, C. Charbonnier, and P. Anschütz. 2013.  
807        Changes in Nutrient Biogeochemistry in Response to the Regression of *Zostera noltii*  
808        Meadows in the Arcachon Bay (France). *Aquatic Geochemistry* 19: 241–259.  
809        doi:10.1007/s10498-013-9192-9

810    Delille, B, AV Borges, and D. Delille. 2009. Influence of giant kelp beds (*Macrocystis pyrifera*)  
811        on diel cycles of pCO<sub>2</sub> and DIC in the sub-Antarctic coastal area. *Estuarine Coastal and*  
812        *Shelf Science* 81: 114–122.

813    De Wit, R. 2008. Microbial diversity in the Bassin d’Arcachon coastal lagoon (SW France).  
814        *Hydrobiologia* 611: 5–15. <https://doi.org/10.1007/s10750-008-9461-6>.

815    Dickson, A.G. and F.J. Millero. 1987. A comparison of the equilibrium constants for the  
816        dissociation of carbonic acid in seawater media. *Deep-Sea Research* 34: 1733–1743.

817 Dickson, A.G. 1990. Standard potential of the reaction:  $\text{AgCl(s)} + 1/2\text{H}_2\text{(g)} = \text{Ag(s)} + \text{HCl(aq)}$ ,  
 818 and the standard acidity constant of the ion  $\text{HSO}_4^-$  in synthetic sea water from 273.15 to  
 819 318.15 K. *Journal of Chemical Thermodynamics* 22: 113–127.

820 Fauvelle, V., A. Belles, H. Budzinski, N. Mazzella, and M. Plus . 2018. Simulated conservative  
 821 tracer as a proxy for S-metolachlor concentration predictions compared to POCIS  
 822 measurements in Arcachon Bay. *Marine Pollution Bulletin* 133: 423–  
 823 427. <https://doi.org/10.1016/j.marpolbul.2018.06.005>.

824 Frankignoulle, M., I. Bourge, C. Canon, and P. Dauby. 1996. Distribution of surface seawater  
 825 partial  $\text{CO}_2$  pressure in the English Channel and in the Southern Bight of the North Sea.  
 826 *Continental Shelf Research* 16: 381–395.

827 Frankignoulle, M., G. Abril, A.V. Borges I. Bourge, C. Canon, B. Delille, E. Libert, and J.M.  
 828 Théate. 1998. Carbon dioxide emission from European estuaries. *Science* 282: 434–436.

829 Frankignoulle, M, A.V. Borges, and R. Biondo. 2001. A new design of equilibrator to monitor  
 830 carbon dioxide in highly dynamic and turbid environments. *Water Research* 35: 344–  
 831 1347.

832 Ganthy, F., A. Sottolichio, R. Verney. 2013. Seasonal modification of tidal flat sediment  
 833 dynamics by seagrass meadows of *Zostera noltii* (Bassin d'Arcachon, France). *Journal*  
 834 *Of Marine Systems* 109: 233–240. <https://doi.org/10.1016/j.jmarsys.2011.11.027>.

835 Gattuso, J.-P., M. Frankignoulle, and R. Wollast. 1998. Carbon and carbonate metabolism in  
 836 coastal aquatic systems. *Annual Review Ecology Systematics* 29, 405–433.

837 Gazeau, F., V.S. Smith, B. Gentili, M. Frankignulle, and J.P. Gattuso. 2004. The European  
 838 coastal zone: characterization and first assessment of ecosystem metabolism, *Estuarine,*  
 839 *Coastal and Shelf Science* 60: 673–694.

840 Gillikin, D.P. and S. Bouillon. 2007. Determination of  $\delta^{18}\text{O}$  of water and  $\delta^{13}\text{C}$  of dissolved  
 841 inorganic carbon using a simple modification of an elemental analyzer—isotope ratio

842 mass spectrometer EA-IRMS: an evaluation. *Rapid Communication in Mass*  
843 *Spectrometry* 21: 1475–1478

844 Glé, C., Y. Del Amo, B. Sautour, P. Laborde, and P. Chardy. 2008. Variability of nutrients and  
845 phytoplankton primary production in a shallow macrotidal coastal ecosystem (Arcachon  
846 Bay, France), *Estuarine, Coastal and Shelf Science* 76 (3): 642–656.

847 Gran, G. 1952. Determination of the equivalence point in potentiometric titrations. Part II.  
848 *Analyst* 77: 661–671.

849 Heijs, S.K., H.M. Jonkers, H. van Gernerden, B.E.M. Schaub, and L.J. Stal. 1999. The  
850 Buffering Capacity Towards Free Sulfide in Sediments of a Coastal Lagoon (Bassin  
851 d’Arcachon, France) the Relative Importance of Chemical and Biological Processes.  
852 *Estuarine, Coastal and Shelf Science* 49 (1): 21–35.  
853 <https://doi.org/10.1006/ecss.1999.0482>.

854 Hu, X., and W.-J. Cai. 2011. An assessment of ocean margin anaerobic processes on oceanic  
855 alkalinity budget. *Global Biogeochemical Cycles* 25: GB3003.  
856 <https://doi.org/10.1029/2010GB003859>.

857 Jähne, B., K.O. Münnich, R. Börsinger, A. Dutzi, W. Huber, and P. Libner. 1987. On the  
858 parameters influencing air-water gas exchange. *Journal of Geophysical Research* 92:  
859 1937-1949.

860 Kjerfve, B. 1985. Comparative oceanography of coastal lagoons. In *Estuarine variability*, ed.  
861 D.A. Wolfe, New York Academic, 63–81.

862 Koné, Y.J., G. Abril, K.N. Kouadio, B. Delille, and A.V. Borges. 2009. Seasonal variability of  
863 carbon dioxide in the rivers and lagoons of Ivory Coast (West Africa). *Estuaries and*  
864 *Coasts* 32: 246–260.

865 Laruelle, G. G, H. H. Durr, C. P. Slomp, and A. V. Borges. 2010. Evaluation of sinks and  
866 sources of CO<sub>2</sub> in the global coastal ocean using a spatially-explicit typology of estuaries

867 and continental shelves. *Geophysical Research Letters* 37, L15607.  
 868 <https://doi.org/10.1029/2010GL043691>.

869 Lazure, P., and F. Dumas. 2008. An external-internal mode coupling for a 3D hydrodynamical  
 870 model for applications at regional scale (MARS). *Advances in water Resources* 31: 233–  
 871 250. <http://doi.org/10.1016/j.advwatres.2007.06.010>.

872 Lee, K., T.W. Kim, R.H. Byrne, F. J. Millero, R. A. Feely, and Y.M. Liu. 2010. The universal  
 873 ratio of boron to chlorinity for the North Pacific and North Atlantic oceans. *Geochimica  
 874 et Cosmochimica Acta* 74: 1801–1811.

875 Lewis, E. and D. Wallace. 1998. Program developed for CO<sub>2</sub> system calculations. *Carbon  
 876 dioxide information analysis center. Oak Ridge National Laboratory*.

877 Maher, D.T., I.R., Santos, L. Golsby-Smith, J. Gleeson, and B.D. Eyre. 2013. Groundwater-  
 878 derived dissolved inorganic and organic carbon exports from a mangrove tidal creek: The  
 879 missing mangrove carbon sink? *Limnology and Oceanography* 58: 1801–1811.  
 880 <https://doi.org/10.4319/lo.2013.58.2.0475>.

881 Mantoura, R. F. C., J. M. Martin, and R. Wollast. 1991. Ocean margin processes. *In Global  
 882 Change, Chichester, UK: Wiley & Sons*, pp. 469.

883 Mehrbach C, C.H. Culberson, J.E. Hawley, and R.N. Pytkowicz. 1973. Measurement of the  
 884 apparent dissociation constants of carbonic acid in seawater at atmospheric pressure.  
 885 *Limnology and Oceanography* 18: 897–907.

886 Migné, A., D. Davoult, N. Spilmont, V. Ouisse, and G. Boucher. 2016. Spatial and temporal  
 887 variability of CO<sub>2</sub> fluxes at the sediment–air interface in a tidal flat of a temperate lagoon  
 888 (Arcachon Bay, France). *Journal of Sea Research*, 109: 13-19.  
 889 <https://doi.org/10.1016/j.seares.2016.01.003>.

890 Miyajima, T., Y. Yamada, Y.T. Hanba, K. Yoshii, T. Koitabashi, and E. Wada. 1995.  
 891 Determining the stable isotope ratio of total dissolved inorganic carbon in lake water by  
 892 GC/C/IRMS. *Limnology and Oceanography* 40: 994–1000.

893 Mook W. G., Koopmans M., Carter A. F., and Keeling C. D. 1983. Seasonal, latitudinal, and  
 894 secular variations in the abundance and isotopic ratios of atmospheric carbon dioxide. 1.  
 895 Results from land stations. *Journal of Geophysical Research* 88: 10915–10933.

896 Neubauer, S. C. and I. C. Anderson. 2003. Transport of dissolved inorganic carbon from a tidal  
 897 freshwater marsh to the York River estuary. *Limnology and Oceanography* 48: 299–307.  
 898 <https://doi.org/10.4319/lo.2003.48.1.0299>.

899 Parker S. R., Poulson S. R., Gammons C. H., and Degrandpre M. D. 2005. Biogeochemical  
 900 controls on diel cycling of stable isotopes of dissolved O<sub>2</sub> and dissolved inorganic carbon  
 901 in the Big Hole River, Montana. *Environmental Science Technology* 39: 7134–7140.

902 Pernetta, J.C. and J.D. Milliman. 1995. Land-Ocean interactions in the coastal zone.  
 903 *Implementation plan, IGPB Rep.* 33: 1–215.

904 Plus, M., F. Dumas, J-Y. Stanisière, and D. Maurer. 2009. Hydrodynamic characterization of  
 905 the Arcachon Bay, using model-derived descriptors. *Continental Shelf Research* 29(8):  
 906 1008-1013. <https://doi.org/10.1016/j.csr.2008.12.016>.

907 Plus, M., S. Dalloyau, G. Trut, I. Auby, X. de Montaudouin, E. Emery, C. Noel, and C. Viala  
 908 2010. Long-term evolution (1988–2008) of *Zostera* spp. Meadows in Arcachon bay (Bay  
 909 of Biscay). *Estuarine, Coastal and Shelf Science* 87: 357–366.

910 Plus, M., I. Auby, D. Maurer, G. Trut, Y. Del Amo, F. Dumas, B. Thouvenin.  
 911 2015. Phytoplankton versus macrophyte contribution to primary production and  
 912 biogeochemical cycles of a coastal mesotidal system. A modelling approach. *Estuarine*  
 913 *Coastal and Shelf Science* 165: 52–60.

914 Polsenaere P., E. Lamaud, J.-M. Bonnefond, V. Lafon, P. Bretel, B. Delille, J. Deborde, D.  
 915 Loustau, and G. Abril. 2012a. Spatial and temporal CO<sub>2</sub> exchanges measured by Eddy  
 916 Covariance over a temperate intertidal flat and their relationships to net ecosystem  
 917 production. *Biogeosciences* 9: 249-268.

918 Polsenaere, P. and G. Abril. 2012. Modelling CO<sub>2</sub> degassing from small acidic rivers using  
 919 water pCO<sub>2</sub>, DIC and  $\delta^{13}\text{C}$ -DIC data. *Geochimica et Cosmochimica Acta* 91: 220-239.

920 Polsenaere P., N. Savoye H. Etcheber M. Canton D. Poirier, S. Bouillon and G. Abril. 2012b.  
 921 Export and degassing of terrestrial carbon through watercourses draining a temperate  
 922 podzolized catchment. *Aquatic Sciences*. <https://doi.org/10.1007/s00027-012-0275-2>.

923 Polsenaere P., R. Lannuzel, S. Guesdon, O. Le Moine, and P. Soletchnik. 2018. Variabilité  
 924 spatio-temporelle des nutriments et du carbone et flux associés le long d'un continuum  
 925 terrestre-aquatique tempéré (Marais poitevin - Baie de l'Aiguillon - Pertuis Breton).  
 926 PROJET AIGUILLON (2016-2020). Rapport scientifique. 85  
 927 pp. <https://archimer.ifremer.fr/doc/00461/57284/>

928 Raymond, P. A. and J. J. Cole. 2001. Gas exchange in rivers and estuaries: choosing a gas  
 929 transfer velocity. *Estuaries* 24: 312–317.

930 Ribas-Ribas, M., A. Gómez-Parra, and J.M. Forja. 2011. Air–sea CO<sub>2</sub> fluxes in the north-  
 931 eastern shelf of the Gulf of Cádiz (southwest Iberian Peninsula). *Marine Chemistry* 123:  
 932 56–66. <https://doi.org/10.1016/j.marchem.2010.09.005>.

933 Ribas-Ribas, M., E. Anfuso, A. Gómez-Parra, and J.M. Forja. 2013. Tidal and seasonal carbon  
 934 and nutrient dynamics of the Guadalquivir estuary and the Bay of Cádiz (SW Iberian  
 935 Peninsula). *Biogeosciences* 10: 4481–4491.

936 Ribaud C., V. Bertrin G. Jan, P. Anschütz, and G. Abril. 2017. Benthic production, respiration,  
 937 and methane oxydation in *Lobelia dormanna* lawns. *Hydrobiologia* 784: 21–34.  
 938 <https://doi.org/10.1007/s10750-016-2848-x>.



939 Rigaud S., B. Deflandre, O. Maire, G. Bernard, and P. Anschütz. 2018. Transient  
 940 biogeochemistry in intertidal sediments: new insights from tidal pools in *Zostera noltei*  
 941 meadows of Arcachon Bay (France). *Marine Chemistry* 200: 1–13.  
 942 <https://doi.org/10.1016/j.marchem.2018.02.002>.

943 Rimmelin, P., J.C. Dumon, E. Maneux, and A. Gonçalves. 1998. Study of annual and seasonal  
 944 dissolved inorganic nitrogen inputs into the Arcachon Lagoon, Atlantic Coast (France).  
 945 *Estuarine Coastal Shelf Science* 47(5): 649–659.

946 Saderne, V., P. Fietzek, and P.M.J., Herman. 2013. Extreme Variations of pCO<sub>2</sub> and pH in a  
 947 Macrophyte Meadow of the Baltic Sea in Summer: Evidence of the Effect of  
 948 Photosynthesis and Local Upwelling. *PLoS One* 8: e62689.

949 Savelli, R., X. Bertin, F. Orvain, P. Gernez, A. Dale, T. Coulombier, P. Pineau, N. Lachaussée,  
 950 P. Polsenaere C. Dupuy, and V. le Fouest. 2019. Impact of chronic and massive  
 951 resuspension mechanisms on the microphytobenthos dynamics in a temperate intertidal  
 952 mudflat. *Journal of Geophysical Research: Biogeosciences* 124. [https://doi.org/10.](https://doi.org/10.1029/2019JG005369)  
 953 1029/2019JG005369.

954 Takahashi, T., S.C. Sutherland, C. Sweeney, A. Poisson, N. Metzl, B. Tilbrook, N. Bates, et al.  
 955 2002. Global sea–air CO<sub>2</sub> flux based on climatological surface ocean pCO<sub>2</sub>, and seasonal  
 956 biological and temperature effects. *Deep Sea Research Part II: Topical Studies in*  
 957 *Oceanography* 49: 1601–1622. [https://doi.org/10.1016/S0967-0645\(02\)00003-6](https://doi.org/10.1016/S0967-0645(02)00003-6).

958 Ternon Q., P. Polsenaere, V. Le Fouest, J.-B. Favier, O. Philippine, J.-M. Chabirand, J. Grizon,  
 959 and C. Dupuy. 2018. Étude des pressions partielles et flux de CO<sub>2</sub> au sein de la  
 960 Communauté d’Agglomération de La Rochelle, rapport scientifique. pp. 32.

961 Vachon, D., Y. T. Prairie, and J. J. Cole. 2010. The relationship between near-surface  
 962 turbulence and gas transfer velocity in freshwater systems and its effect on floating  
 963 chamber measurements. *Limnology and Oceanography* 55: 1723–1732.

964 Vaz, L., Frankenbach, S., Serôdio, J., Dias, J.M. 2019. New insights about the primary  
 965 production dependence on abiotic factors: Ria de Aveiro case study. *Ecological*  
 966 *Indicators*: 106, 105555, ISSN 1470-160X,  
 967 <https://doi.org/10.1016/j.ecolind.2019.105555>.

968 Wang, Z. A. and W.-J. Cai. 2004. Carbon dioxide degassing and inorganic carbon export from  
 969 a marsh-dominated estuary (the Dublin River): a marsh CO<sub>2</sub> pump. *Limnology and*  
 970 *Oceanography* 49: 341–354.

971 Wang, Z.A., K.D. Kroeger, N.K. Ganju, M.E. Gonneea, and S.N. Chu. 2016. Intertidal salt  
 972 marshes as an important source of inorganic carbon to the coastal ocean. *Limnology and*  
 973 *Oceanography* 61: 1916–1931. <https://doi.org/10.1002/lno.10347>.

974 Wang, S.R., D. Di Iorio, W.-J. Cai, and C.S. Hopkinson. 2018. Inorganic carbon and oxygen  
 975 dynamics in a marsh-dominated estuary. *Limnology and Oceanography* 63: 47-71.  
 976 <https://doi.org/10.1002/lno.10614>.

977 Wanninkhof, R. 1992. Relationship between gas exchange and wind speed over the ocean.  
 978 *Journal of Geophysical Research* 97: 7373–7382.

979 Weiss, R.F. 1974. Carbon dioxide in water and seawater: the solubility of a non-ideal gas.  
 980 *Marine Chemistry* 2: 203–215.

981 Yang C., Telmer K., and Veizer J. 1996. Chemical dynamics of the ‘St. Lawrence’ riverine  
 982 system:  $\delta\text{H}_2\text{O}$ ,  $\delta^{18}\text{OH}_2\text{O}$ ,  $\delta^{13}\text{CDIC}$ ,  $\delta^{34}\text{SSulfate}$ , and Dissolved  $^{87}\text{Sr}/^{86}\text{Sr}$ . *Geochimica*  
 983 *Cosmochimica Acta* 60: 851–866.

984 Yates, K. K., C. Dufore, N. Smiley, C. Jackson, and R. B. Halley. 2007. Diurnal variation of  
 985 oxygen and carbonate system parameters in Tampa Bay and Florida Bay. *Marine*  
 986 *Chemistry* 104: 110–124.

987 Zemmeling, H. J., H.A. Slagter, C. van Slooten, J. Snoek, B. Heusinkveld, J. Elbers, N.J. Bink,  
 988 W. Klaassen, C. J. M. Philippart, and H. J. W. de Baar. 2009. Primary production and

eddy correlation measurements of CO<sub>2</sub> exchange over an intertidal estuary. *Geophysical Research Letters* 36: LI19606. <https://doi.org/10.1029/2009GL039285>.

Zhang, L., M. Xue, and Q. Liu. 2012. Distribution and seasonal variation in the partial pressure of CO<sub>2</sub> during autumn and winter in Jiaozhou Bay, a region of high urbanization. *Marine Pollution Bulletin* 64: 56–65.

## Figure/Table captions

**Table 1** Inorganic carbon parameters measured during eight 24 hour-cycles to six 24h and two 12h cycles in the Arcachon flat (44°42.400'N 01°07.500'W) (number of values, mean ± standard deviation in bold and range between brackets). T and S water temperature and salinity, δ<sup>13</sup>C-DIC dissolved inorganic carbon isotopic ratio, TA total alkalinity, pCO<sub>2</sub> partial pressure of CO<sub>2</sub>, and DIC dissolved inorganic carbon. DIC were estimated from measured salinity, temperature, TA and pCO<sub>2</sub> values using the CO<sub>2</sub> system calculation program (Lewis and Wallace 1998) parameterized with the carbonic acid constants sets proposed by Mehrbach et al. (1973) refitted by Dickson and Millero (1987), the borate acidity constant from Lee et al. (2010) and the CO<sub>2</sub> solubility coefficient of Weiss (1974). 15/04/2008 10:00:00 (TU) – 16/04/2008 10:00:00, 02/07/2008 10:00 – 03/07/2008 10:00, 18/09/2008 11:00 – 19/09/2008 11:00, 06/11/2008 08:00 – 06/11/2008 17:00, 29/01/2009 06:00 – 29/01/2009 14:00, 15/04/2009 13:00 – 16/04/2009 13:00, 25/06/2009 06:00 – 26/06/2009 06:00 and 04/09/2009 05:00 – 05/09/2009 05:00. Notice that November 2008 and January 2009 were 12 hour-cycles

**Table 2** Gas transfer velocities (k<sub>600</sub>) and air-sea CO<sub>2</sub> fluxes computed at high tide day and night periods (Fig. 3, the four-hour emerged-periods around low tide at each cycle were removed) for each cycle in the Arcachon flat (mean ± standard deviation and range between

brackets).  $U_{10}$  values were computed from wind speed values measured at 9 meters high by the Lège-Cap Ferret Meteo-France station, 12 km far from the 24-H site) using the Amorochio and DeVries (1980) equation.  $k_{600}$  values were estimated according to Wanninkhof et al. (1992), Raymond & Cole (2001) and Abril et al. (2009) equations (W92, RC01 and A09, respectively, see M&M). Air-sea  $CO_2$  fluxes were then calculated from  $k_{600}$ , water and air  $pCO_2$  values. A mean air  $pCO_2$  value of 390 ppm was chosen according to Eddy Covariance (EC) measurements deployed at 1.8 km far from the tidal creek in 2008 and 2009 (Polsenaere et al. 2012a). For comparison,  $U_{10}$  and air-sea  $CO_2$  flux values obtained in July 2008 from simultaneous EC measurements (Polsenaere et al. 2012a) in July 2008 are shown in red. No  $k_{600}$  calculations were attempted from these simultaneous EC flux and water  $pCO_2$  measurements at this season due to strong spatial heterogeneity in water bodies highlighted in the present study (see Discussion section 4.4.2.)

**Table 3** Seasonal, tidal and diurnal  $pCO_2$  and water-atmosphere variation comparisons across tidal flat, bay, marsh-estuary and mangrove systems of the coastal zone (<sup>a</sup>diurnal and/or tidal, <sup>b</sup>spatial and/or longitudinal sampling methodology)

**Table 4** Comparison between day and night  $pCO_2$  values averaged over a same salinity range according to tidal phases (flooding/ebbing) for each 2008-2009 cycle. The non-parametric Mann-Whitney (p-values: \*\*\* = 0.0002; \*\*\*\* < 0.0001) test was used. / symbol indicates cycles (flooding and/or ebbing periods) where comparisons were not possible due to not enough data (no data > 5 min. with no significant salinity value difference between day and night periods). To the contrary, time periods (min.) (> 5 min.) where comparisons were possible are specified for each cycle. Temperature comparisons are also given along with the  $pCO_2$  increase or decrease only due to day through nighttime temperature difference (calculated with the  $CO_2$

System Calculation program (version 2.1.) (Lewis and Wallace 1998) from constant T, S, TA and DIC values measured during each cycle (see Table 1 and M&M section)

**Fig. 1** Localization of the 24 hour-cycle site. (a) The Arcachon lagoon with the subtidal zone (channels and creeks) and the intertidal mudflat area; (b) the 24 hour-cycle site (24H, 44°42.400'N 01°07.500'W in the subtidal creek always immersed); the EC station (EC, 44°42.9858'N 01°08.6160'W, 1.8 km far from the 24-H site, in the intertidal area emerged for approximately four hours and immersed for approximately nine hours, Polsenaere et al. 2012a); the meteo-france station (A) (MF, 44°37.900'N 01°14.900'W, 12.450 km far from the 24-H site). The *Zostera noltei* seagrass meadow is derived from the SPOT image of the 22 June 2005; it occupies 60 % of the intertidal area (shades of green show the differences in seagrass density, brown and yellow represent muddy and sandy areas)

**Fig. 2** *In situ* water temperatures (dashed black curve), pCO<sub>2</sub> (black curve with black dots) and derived temperature-normalized pCO<sub>2</sub> (NpCO<sub>2</sub>, i.e. pCO<sub>2</sub> variations due to biological activity or non-temperature effects, black dotted curve with empty black dots, annual mean temperature over 2008/09  $17.7 \pm 4.2^{\circ}\text{C}$ , dotted line) and thermally forced seasonal pCO<sub>2</sub> according to Takahashi et al. (2002) (TpCO<sub>2</sub>, i.e. pCO<sub>2</sub> variations due to thermal effects, grey dotted curve with grey dots, annual mean temperature over 2008/09,  $17.7 \pm 4.2^{\circ}\text{C}$ , dotted line and pCO<sub>2</sub>  $496 \pm 36$  ppmv, dashed line); mean temperature and pCO<sub>2</sub> over the whole 2008 and 2009 period were chosen for NpCO<sub>2</sub> and TpCO<sub>2</sub> computations due to sampled cycle strategy and for better consistency in year comparisons. Minimum and maximum pCO<sub>2</sub> values (associated to the mean pCO<sub>2</sub> value) measured during each tidal cycle are also represented (vertical black lines)

**Fig. 3** Tidal and diurnal variations in inorganic carbon and associated parameters measured during eight 24 hour-cycles to six 24h and two 12h cycles in the Arcachon flat. Water height (H), salinity (S), temperature (T), partial pressure of CO<sub>2</sub> in the water (pCO<sub>2</sub>), total alkalinity (TA), dissolved inorganic carbon (DIC) and dissolved inorganic carbon isotopic ratio ( $\delta^{13}\text{C}$ -DIC); (a) 15/04/2008 10:00:00 (TU) – 16/04/2008 10:00:00, (b) 02/07/2008 10:00 – 03/07/2008 10:00, (c) 18/09/2008 11:00 – 19/09/2008 11:00, (d) 06/11/2008 08:00 – 06/11/2008 17:00, (e) 29/01/2009 06:00 – 29/01/2009 14:00, (f) 15/04/2009 13:00 – 16/04/2009 13:00, (g) 25/06/2009 06:00 – 26/06/2009 06:00 and (h) 04/09/2009 05:00 – 05/09/2009 05:00. T and S were measured every minute by the YSI multiparameter probe on board and H was measured every hour by the SHOM. The other parameters were sampled on board every hour. Clear and grey areas represent daytime and nighttime periods, respectively. Notice the same y-axis scale between cycles was chosen to better see seasonal variations and that November 2008 and January 2009 were 12 hour-cycles

**Fig. 4** Cross-correlation plots of TA (a), DIC (c) and  $\delta^{13}\text{C}$ -DIC (d) values versus salinity and apparent 0 end-member versus *in situ* catchment TA value comparison (b). TA versus S slopes are all significantly positive, DIC versus S slopes are significantly positive except in September 2009 (negative); and  $\delta^{13}\text{C}$ -DIC versus S slopes are positive and significant except in April 2008, November 2008, September 2009. (b) Apparent 0 end-member TA and *in situ* catchment TA correspond to Y-intercept of TA versus S cross-correlations and *in situ* TA measurements carried out at the same time over the Arcachon lagoon watershed watercourses (see Polsenaere et al. 2012b) computed here as discharge-weighted TA means, respectively

**Fig. 5** Diurnal/tidal plots of water temperature and pCO<sub>2</sub> versus salinity for the four periods: HT\_N high tide at night (dark blue triangle), LT\_N low tide at night (green inversed triangle),

LT\_D low tide at day (yellow inversed triangle) and HT\_D high tide at day (clear blue triangle). (a, b) April 2008, (c, d) July 2008, (e, f) September 2008, (g, h) November 2008, (I, j) January 2009, (k, l) April 2009, (m, n) June 2009 and (o, p) September 2009. Notice the same y-axis pCO<sub>2</sub> scale between all cycles was chosen to better observe diurnal and tidal variations. The same x-axis temperature and salinity scales between April 2008-2009, July 2008-June 2009 and September 2008-2009 were also chosen to better observe variations during the same seasons from 2008 to 2009

**Table 1**

	<i>T</i> (°C)	<i>S</i>	δ <sup>13</sup> C-DIC (‰)	TA (mmol kg <sup>-1</sup> )	pCO <sub>2</sub> (ppmv)	DIC (mmol kg <sup>-1</sup> )
<i>April 2008</i>	<i>1441</i>	<i>1441</i>	<i>23</i>	<i>25</i>	<i>1441</i>	<i>25</i>
	<b>13.9 ± 0.6</b>	<b>29.2 ± 0.6</b>	<b>-1.1 ± 1.1</b>	<b>2.081 ± 0.028</b>	<b>474 ± 14</b>	<b>1.948 ± 0.024</b>
	(12.8 ~ 15.4)	(26.2 ~ 30.1)	(-3.7 ~ -0.4)	(2.000 ~ 2.119)	(442 ~ 496)	(1.884 ~ 1.985)
<i>July 2008</i>	<i>1464</i>	<i>1464</i>	<i>24</i>	<i>25</i>	<i>1434</i>	<i>25</i>
	<b>22.2 ± 0.6</b>	<b>31.2 ± 0.6</b>	<b>-0.5 ± 0.4</b>	<b>2.131 ± 0.035</b>	<b>461 ± 14</b>	<b>1.926 ± 0.028</b>
	(21.2 ~ 23.4)	(30.2 ~ 32.6)	(-1.7 ~ 0.2)	(2.072 ~ 2.211)	(432 ~ 499)	(1.879 ~ 1.995)
<i>September 2008</i>	<i>1428</i>	<i>1428</i>	<i>25</i>	<i>25</i>	<i>1436</i>	<i>25</i>
	<b>19.2 ± 0.2</b>	<b>33.6 ± 0.3</b>	<b>-0.6 ± 0.3</b>	<b>2.255 ± 0.021</b>	<b>515 ± 36</b>	<b>2.062 ± 0.017</b>
	(18.8 ~ 20.2)	(33.1 ~ 34.5)	(-1.5 ~ -0.1)	(2.223 ~ 2.301)	(405 ~ 597)	(2.017 ~ 2.086)
<i>November 2008</i>	<i>541</i>	<i>541</i>	<i>10</i>	<i>10</i>	<i>541</i>	<i>10</i>
	<b>12.3 ± 0.2</b>	<b>32.2 ± 0.3</b>	<b>-0.6 ± 0.3</b>	<b>2.202 ± 0.020</b>	<b>463 ± 19</b>	<b>2.050 ± 0.022</b>
	(12.0 ~ 12.6)	(31.8 ~ 32.6)	(-1.3 ~ -0.3)	(2.180 ~ 2.234)	(419 ~ 497)	(2.021 ~ 2.081)
<i>January 2009</i>	<i>490</i>	<i>480</i>	<i>9</i>	<i>9</i>	<i>480</i>	<i>9</i>
	<b>8.9 ± 0.4</b>	<b>23.2 ± 1.5</b>	<b>-1.0 ± 0.5</b>	<b>1.646 ± 0.086</b>	<b>480 ± 15</b>	<b>1.594 ± 0.076</b>
	(8.3 ~ 10.3)	(20.4 ~ 25.6)	(-2.1 ~ -0.5)	(1.493 ~ 1.733)	(452 ~ 503)	(1.458 ~ 1.669)
<i>April 2009</i>	<i>1518</i>	<i>1518</i>	<i>25</i>	<i>25</i>	<i>1518</i>	<i>25</i>
	<b>13.7 ± 0.3</b>	<b>30.1 ± 1.0</b>	<b>-0.7 ± 0.1</b>	<b>2.006 ± 0.053</b>	<b>525 ± 14</b>	<b>1.891 ± 0.045</b>
	(12.7 ~ 14.5)	(24.8 ~ 31.5)	(-0.9 ~ -0.5)	(1.840 ~ 2.101)	(494 ~ 568)	(1.752 ~ 1.968)
<i>June 2009</i>	<i>1441</i>	<i>1441</i>	<i>24</i>	<i>25</i>	<i>1441</i>	<i>25</i>

	<b>21.5 ± 0.6</b> (20.0 ~ 23.3)	<b>31.0 ± 0.4</b> (30.2 ~ 32.2)	<b>-0.2 ± 0.2</b> (-0.4 ~ 0.2)	<b>2.099 ± 0.029</b> (2.044 ~ 2.156)	<b>490 ± 27</b> (419 ~ 545)	<b>1.916 ± 0.023</b> (1.866 ~ 1.951)
<i>September 2009</i>	<i>1441</i>	<i>1440</i>	<i>25</i>	<i>25</i>	<i>1435</i>	<i>25</i>
	<b>20.9 ± 0.3</b> (20.2 ~ 21.5)	<b>34.0 ± 0.3</b> (33.5 ~ 34.8)	<b>-0.2 ± 0.3</b> (-0.90 ~ 0.4)	<b>2.218 ± 0.020</b> (2.187 ~ 2.251)	<b>530 ± 39</b> (453 ~ 601)	<b>2.021 ± 0.021</b> (1.978 ~ 2.051)
<i>2008-2009</i>	<i>9764</i>	<i>9753</i>	<i>165</i>	<i>169</i>	<i>9726</i>	<i>169</i>
<i>Average</i>	<b>17.7 ± 4.2</b> (8.3 ~ 23.4)	<b>30.5 ± 3.4</b> (20.4 ~ 34.8)	<b>-0.6 ± 0.4</b> (-3.7 ~ 0.4)	<b>2.079 ± 0.036</b> (1.493 ~ 2.301)	<b>496 ± 36</b> (405 ~ 601)	<b>1.926 ± 0.032</b> (1.458 ~ 2.086)

1105  
1106  
1107  
1108



Table 2

		$U_{10}$ (m s <sup>-1</sup> )	$K_{600}$ (cm h <sup>-1</sup> )	Air-Sea CO <sub>2</sub> fluxes (mmol m <sup>-2</sup> h <sup>-1</sup> )				
			W92	RC01	A09	W92	RC01	A09
<b>Apr. 08</b>	<i>Day</i>	<b>4.42 ± 1.42</b> (2.02 ~ 6.06)	<b>6.59 ± 3.71</b> (1.26 ~ 11.37)	<b>9.9 ± 4.46</b> (3.87 ~ 15.91)	<b>17.04 ± 4.92</b> (8.76 ~ 22.74)	<b>0.19 ± 0.1</b> (0.05 ~ 0.34)	<b>0.29 ± 0.12</b> (0.14 ~ 0.48)	<b>0.5 ± 0.12</b> (0.32 ~ 0.69)
	<i>Night</i>	<b>2.88 ± 0.7</b> (2.02 ~ 4.04)	<b>2.71 ± 1.27</b> (1.26 ~ 5.05)	<b>5.38 ± 1.34</b> (3.87 ~ 7.85)	<b>11.74 ± 2.4</b> (8.76 ~ 15.72)	<b>0.07 ± 0.04</b> (0.02 ~ 0.14)	<b>0.13 ± 0.05</b> (0.07 ~ 0.22)	<b>0.29 ± 0.11</b> (0.16 ~ 0.44)
<b>Jul. 08</b>	<i>Day</i>	<b>4.46 ± 2.34</b> (2.02 ~ 11.1)	<b>7.71 ± 9.88</b> (1.26 ~ 38.21)	<b>14.92 ± 24.73</b> (3.87 ~ 93.05)	<b>17.16 ± 8.06</b> (8.69 ~ 40.09)	<b>0.18 ± 0.23</b> (0.03 ~ 0.9)	<b>0.36 ± 0.58</b> (0.09 ~ 2.19)	<b>0.41 ± 0.2</b> (0.2 ~ 0.94)
	<i>Night</i>	<b>5.05 ± 1.43</b> (3.03 ~ 6.06)	<b>8.37 ± 4.03</b> (2.84 ~ 11.37)	<b>12.12 ± 4.94</b> (5.51 ~ 15.91)	<b>19.2 ± 4.91</b> (12.24 ~ 22.68)	<b>0.21 ± 0.11</b> (0.07 ~ 0.31)	<b>0.31 ± 0.13</b> (0.14 ~ 0.43)	<b>0.49 ± 0.13</b> (0.32 ~ 0.61)
EC data Tidal flat	<i>Day</i>	<b>3.86 ± 1.29</b> (1.29 ~ 7.71)				<b>-2.25 ± 2.7</b> (-12.38 ~ 2.1)		
	<i>Night</i>	<b>4.3 ± 2.21</b> (0.69 ~ 10.14)				<b>0.12 ± 1.37</b> (-2.56 ~ 1.76)		
<b>Sep. 08</b>	<i>Day</i>	<b>2.48 ± 0.83</b> (1.01 ~ 4.04)	<b>2.1 ± 1.33</b> (0.32 ~ 5.05)	<b>4.72 ± 1.41</b> (2.72 ~ 7.85)	<b>10.32 ± 2.86</b> (5.24 ~ 15.73)	<b>0.08 ± 0.05</b> (0.01 ~ 0.16)	<b>0.19 ± 0.06</b> (0.1 ~ 0.3)	<b>0.42 ± 0.15</b> (0.2 ~ 0.68)
	<i>Night</i>	<b>2.31 ± 1.39</b> (1.01 ~ 5.05)	<b>2.17 ± 2.66</b> (0.32 ~ 7.9)	<b>4.82 ± 2.95</b> (2.72 ~ 11.17)	<b>9.76 ± 4.81</b> (5.29 ~ 19.22)	<b>0.08 ± 0.11</b> (0.01 ~ 0.32)	<b>0.19 ± 0.12</b> (0.09 ~ 0.45)	<b>0.38 ± 0.19</b> (0.2 ~ 0.78)
<b>Nov. 08</b>	<i>Day</i>	<b>7.74 ± 1.77</b> (5.05 ~ 10.09)	<b>19.37 ± 8.37</b> (7.9 ~ 31.58)	<b>33.33 ± 19.51</b> (11.17 ~ 65.36)	<b>28.38 ± 6.12</b> (19.08 ~ 36.54)	<b>0.53 ± 0.22</b> (0.25 ~ 0.87)	<b>0.92 ± 0.52</b> (0.36 ~ 1.81)	<b>0.79 ± 0.14</b> (0.61 ~ 1.01)
	<i>Night</i>							
<b>Jan. 09</b>	<i>Day</i>	<b>2.27 ± 0.97</b> (1.01 ~ 3.03)	<b>1.82 ± 1.25</b> (0.32 ~ 2.84)	<b>4.4 ± 1.36</b> (2.72 ~ 5.51)	<b>9.58 ± 3.3</b> (5.27 ~ 12.19)	<b>0.06 ± 0.04</b> (0.01 ~ 0.11)	<b>0.14 ± 0.06</b> (0.08 ~ 0.21)	<b>0.29 ± 0.13</b> (0.16 ~ 0.46)
	<i>Night</i>							
<b>Apr. 09</b>	<i>Day</i>	<b>5.35 ± 3.37</b> (1.01 ~ 10.09)	<b>12.03 ± 12.55</b> (0.32 ~ 31.58)	<b>22.84 ± 25.61</b> (2.72 ~ 65.36)	<b>20.02 ± 11.43</b> (5.24 ~ 36.09)	<b>0.56 ± 0.59</b> (0.01 ~ 1.59)	<b>1.06 ± 1.2</b> (0.12 ~ 3.3)	<b>0.93 ± 0.55</b> (0.23 ~ 1.82)
	<i>Night</i>	<b>4.04 ± 1.81</b> (2.02 ~ 7.07)	<b>5.9 ± 5.23</b> (1.26 ~ 15.48)	<b>9.43 ± 6.95</b> (3.87 ~ 22.65)	<b>15.58 ± 6.18</b> (8.65 ~ 25.9)	<b>0.23 ± 0.2</b> (0.06 ~ 0.6)	<b>0.38 ± 0.26</b> (0.18 ~ 0.87)	<b>0.63 ± 0.21</b> (0.4 ~ 1)
<b>Jun. 09</b>	<i>Day</i>	<b>3.62 ± 1.32</b> (1.01 ~ 5.05)	<b>4.55 ± 2.65</b> (0.32 ~ 7.9)	<b>7.39 ± 2.92</b> (2.72 ~ 11.17)	<b>14.18 ± 4.51</b> (5.25 ~ 19.06)	<b>0.13 ± 0.08</b> (0.01 ~ 0.25)	<b>0.22 ± 0.09</b> (0.09 ~ 0.35)	<b>0.43 ± 0.14</b> (0.17 ~ 0.6)
	<i>Night</i>	<b>3.7 ± 1.17</b> (3.03 ~ 5.05)	<b>4.53 ± 2.92</b> (2.84 ~ 7.9)	<b>7.4 ± 3.27</b> (5.51 ~ 11.17)	<b>14.54 ± 4.02</b> (12.21 ~ 19.18)	<b>0.12 ± 0.08</b> (0.07 ~ 0.22)	<b>0.2 ± 0.09</b> (0.13 ~ 0.31)	<b>0.4 ± 0.12</b> (0.29 ~ 0.53)
<b>Sep. 09</b>	<i>Day</i>	<b>9.31 ± 3.1</b> (5.05 ~ 13.12)	<b>29.51 ± 18.64</b> (7.9 ~ 53.37)	<b>81.73 ± 80.78</b> (11.17 ~ 188.61)	<b>32.09 ± 10.07</b> (19.18 ~ 46.85)	<b>1.02 ± 0.65</b> (0.23 ~ 1.83)	<b>2.8 ± 2.68</b> (0.32 ~ 6.48)	<b>1.11 ± 0.47</b> (0.48 ~ 1.65)
	<i>Night</i>	<b>2.88 ± 0.91</b> (2.02 ~ 4.04)	<b>2.8 ± 1.7</b> (1.26 ~ 5.05)	<b>5.48 ± 1.78</b> (3.87 ~ 7.85)	<b>11.71 ± 3.14</b> (8.71 ~ 15.75)	<b>0.11 ± 0.06</b> (0.05 ~ 0.21)	<b>0.23 ± 0.06</b> (0.14 ~ 0.33)	<b>0.49 ± 0.11</b> (0.32 ~ 0.66)

**Table 3**

Study Site	Seasonal pCO <sub>2</sub> range (ppmv)	Diurnal-tidal pCO <sub>2</sub> range (ppmv)	Water-atmosphere CO <sub>2</sub> flux (mmol m <sup>-2</sup> h <sup>-1</sup> )	Reference
Arcachon tidal flat (France)	461 ± 14 (July 2008) – 530 ± 39 (September 2009)	(452 - 503) (January 2009) to (405 - 597) (September 2008)	0.27 ± 0.22 to 0.56 ± 0.54	This study <sup>a</sup>
Aiguillon tidal flat (France)	(390 - 609) (spring - summer 2017) (215 - 1929) (summer - fall 2018)		0.14 (-0.075 to 1.13, summer - winter)	Polsenaere et al. (2018) <sup>b</sup> ; Coignot et al. (2020; in prep.) <sup>b</sup>
Aiguillon tidal flat (France)		(466 - 1024) (HT-LT) (summer 2018)	1.00 ± 0.82	Ternon et al. (2018) <sup>a</sup>
Duplin River salt marsh-estuary (Georgia, USA)		(500 - 4000) (HT-LT, winter) to (1600 - 12,000) (HT-LT, summer) (2014)	-0.7 to -5.5 and -0.6 to -3.9	Wang et al. (2018) <sup>a,b</sup>
Tidal marsh channel of the Fier d'Ars (Ré Island, France)	385 ± 60 (267 - 522) (summer) to 460 ± 58 (334 - 569) (autumn)	(377 - 510) (HT-LT, winter 2018) to (334 - 569) (HT - LT, Autumn 2018)	-0.18 ± 0.18 (spring) to 0.10 ± 0.08 (winter)	Mayen et al. (in prep.) <sup>a</sup>
Amazon estuary - tidal forest channel		5000 ± 300 - 2320 ± 40 (LT - HT, February 2007)		Abril et al. (2013) <sup>a</sup>
Ras Dege (Tanzania) mangrove creek		500 - 5000 (September 2005)	0.04-3.33	Bouillon et al. (2007) <sup>a</sup>
Nagada (Papua New Guinea) and the Gaderu (India) mangrove creeks		(540 - 1680) and (1380 - 4770) (July, August 2000)	1.82 ± 1.38 and 2.33 ± 4.20	Borges et al. (2003) <sup>a</sup>
Bay of Brest (subtidal)	200 - 700 (summer-winter, 2013 to 2010)		-0.0083 to -0.38 (spring and summer) and 0.038 to 0.91 (fall and winter)	Bozec et al. (2011) <sup>a</sup>
Estuary of Guadalquivir	341 ± 18 (February 2007) - 411 ± 20 (November 2006)		-0.058 (February 2007) and 0.15 (November 2006)	Ribas-Ribas et al. (2011) <sup>b</sup>
Estuary and the Bay of Cadiz		(589 - 1244), (525 - 1405) and (742 - 1059) (HT-LT, summer 2015)	0.375 to 2.37	Burgos et al. (2018) <sup>a,b</sup>
Coastal systems of Cadiz Bay (Spain)				
Jiaozhou Bay (East China Sea)	315 - 720 (autumn 2007) and 145 - 315 (winter 2008)		0.12 (autumn) and -0.68 (winter)	Zhang et al. (2012) <sup>b</sup>
Tampa and Florida bays (US)	414 ± 86 (October 2003); 351 ± 72 (March 2000)	(262 - 580) (October 2003); (260 - 497) (March 2000)		Yates et al. (2007) <sup>a</sup>
Macrophyte meadow (Baltic Sea)		281 ± 88 (July); 219 ± 24 (August); 1488 ± 574 (September 2011)		Saderne et al. (2013) <sup>a</sup>
<i>Zostera marina</i> meadow, Eastern shore of Virginia (US)	425 (April) - 490 (June 2015)	(193 - 731) (April); (256 - 859) (June 2015)		Berg et al. (2019) <sup>a</sup>
Guanabara Bay (Brazil)	353 ± 141 and 194 ± 127 (S3); 380 ± 286 and 203 ± 159 (S4); 364 ± 343 and 132 ±	591 ± 231 to 194 ± 114 (September 2013); 163 ± 40 to 116 ± 25 (January 2014); 346 ± 166 to 146	-2.87 (S3); -2.16 (S4); -2.52 (S5)	Cotovicz et al. (2015) <sup>a,b</sup>

74 (S5) (winter and summer) ± 106 (February 2014);  
637 ± 421 to 265 ± 186  
(April 2014) (S4, S5)

**Table 4**

		Day			Night			Significant differences (Day vs Night)			pCO <sub>2</sub> increase or decrease only due to day through night T difference
		Salinity	pCO <sub>2</sub> (ppmv)	T (°C)	Salinity	pCO <sub>2</sub> (ppmv)	T (°C)	Salinity	pCO <sub>2</sub>	T	
<i>Apr.</i>	<b>Flooding</b>	/	/	/	/	/	/	/	/	/	/
<i>2008</i>	<b>Ebbing (30 min.)</b>	29.27	481	14.4 7	29.27	471	13.5 6	No	Yes ****	Yes ****	-18
<i>Jul.</i>	<b>Flooding</b>	/	/	/	/	/	/	/	/	/	/
<i>2008</i>	<b>Ebbing (10 min.)</b>	30.4	493	21.3 5	30.43	471	22.5 5	No	Yes ****	Yes ****	+21
<i>Sept.</i>	<b>Flooding (120 min.)</b>	33.55	513	18.9 5	33.55	537	19.0 7	No	Yes ****	Yes ****	+2
	<b>Ebbing</b>	/	/	/	/	/	/	/	/	/	/
<i>Nov.</i>	<b>Flooding</b>	/	/	/	/	/	/	/	/	/	/
<i>2008</i>	<b>Ebbing</b>	/	/	/	/	/	/	/	/	/	/
<i>Jan.</i>	<b>Flooding</b>	/	/	/	/	/	/	/	/	/	/
<i>2009</i>	<b>Ebbing</b>	/	/	/	/	/	/	/	/	/	/
<i>Apr.</i>	<b>Flooding</b>	/	/	/	/	/	/	/	/	/	/
<i>2009</i>	<b>Ebbing</b>	/	/	/	/	/	/	/	/	/	/
<i>Jun.</i>	<b>Flooding</b>	/	/	/	/	/	/	/	/	/	/
<i>2009</i>	<b>Ebbing</b>	/	/	/	/	/	/	/	/	/	/
<i>Sept.</i>	<b>Flooding (30 min.)</b>	33.89	552	20.9 7	33.9	572	20.5 8	No	Yes ***	Yes ****	-8
<i>2009</i>	<b>Ebbing (15 min.)</b>	33.97	540	20.9 7	33.96	535	20.8 4	No	Yes ***	Yes ****	-3

**Fig. 1**

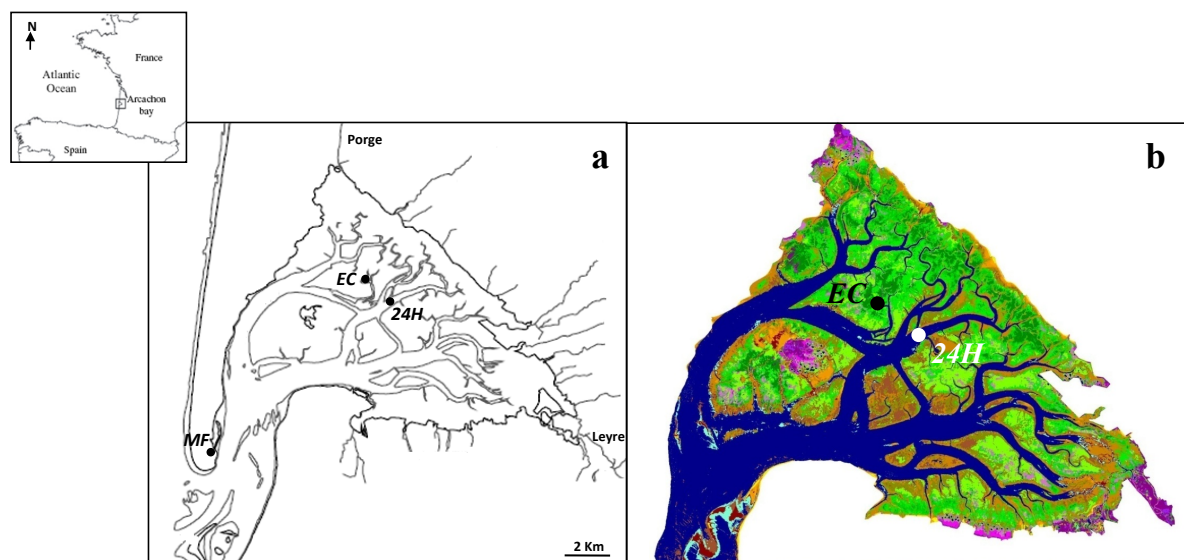
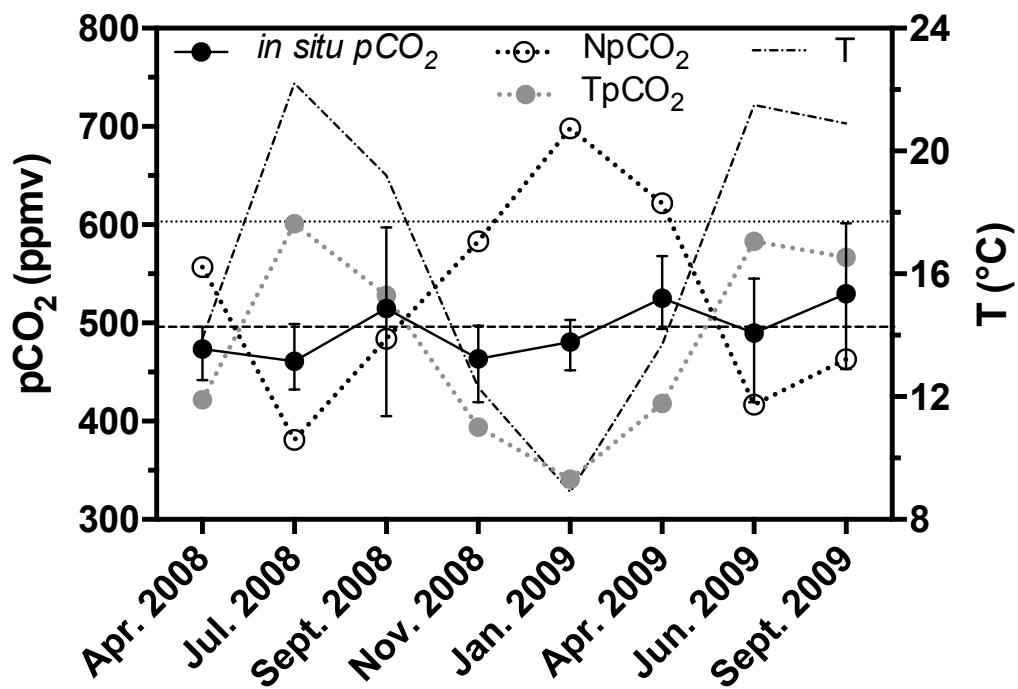


**Fig. 2**



1199  
1200  
1201  
1202  
1203  
1204  
1205  
1206  
1207  
1208  
1209  
1210

**Fig. 3**

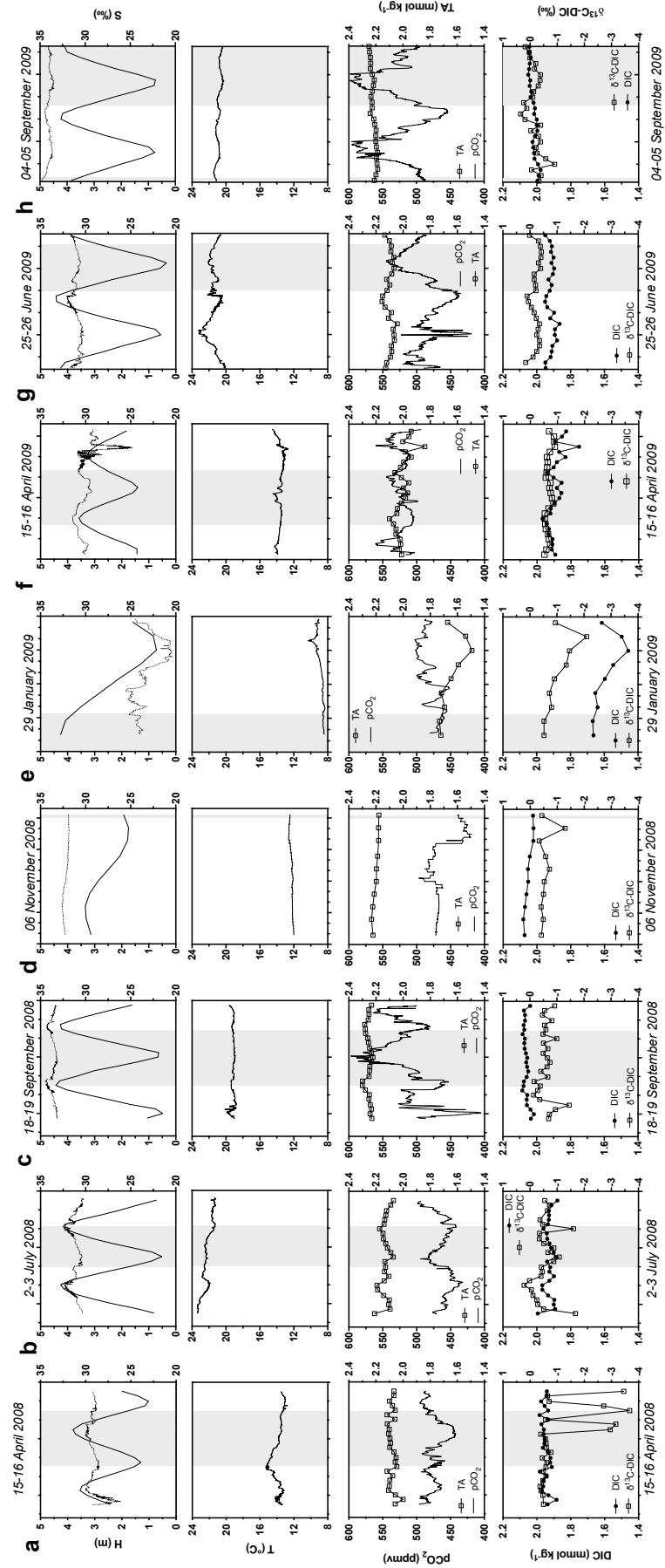


Fig. 4

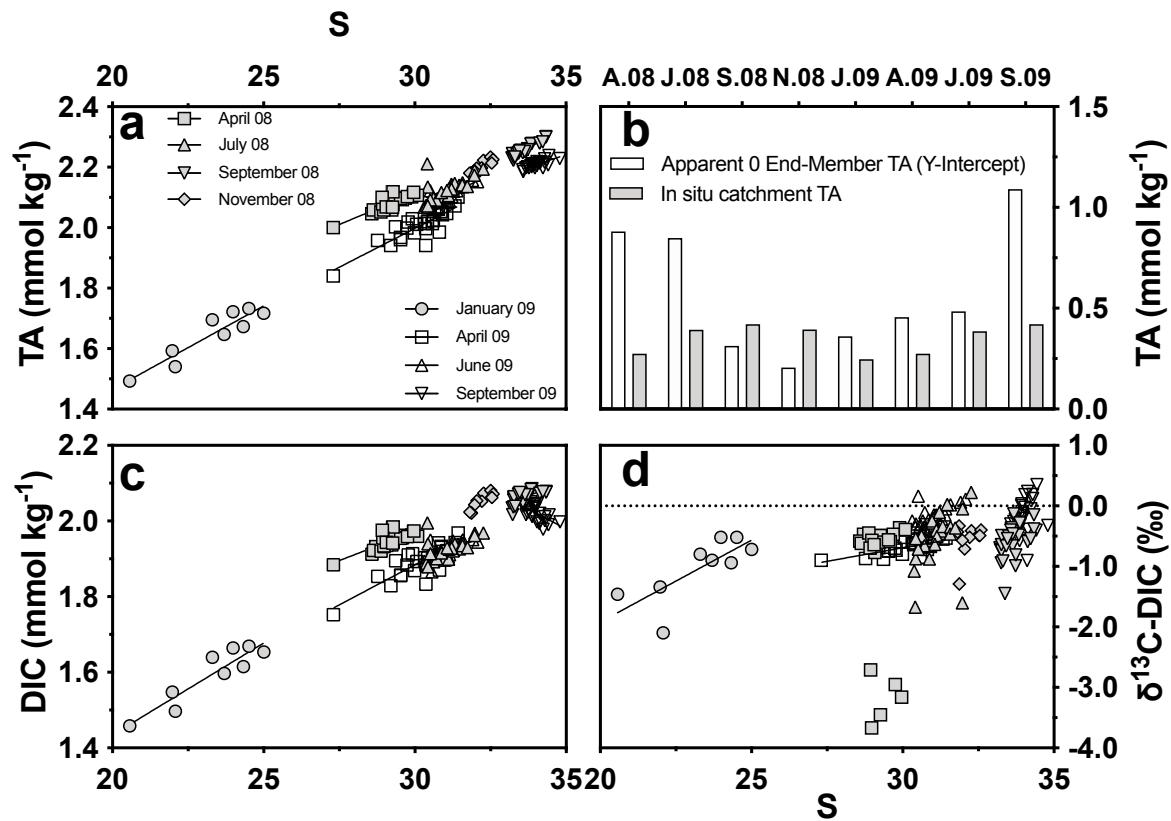


Fig. 5



